PART II

SIMULATION

3

MATHEMATICAL MODELS FOR THE FILLING AND PACKING SIMULATION

HUAMIN ZHOU, ZIXIANG HU, and DEQUN LI

State Key Laboratory of Materials Processing and Die & Mould Technology, Huazhong University of Science and Technology, Wuhan, Hubei, China

In this chapter, material properties and governing equations for fluid flow in the filling and packing phases of injection molding process will be introduced first, and then boundary conditions and some mold simplifications will be presented.

At present, the mathematical description generally bases on the continuum assumption,[1−3] on which the governing equations are premised, including mass conservation equation, momentum conservation equations, energy conservation equation, and constitutive equation reflecting the material properties. According to the characteristics of the problem, the governing equations can be simplified appropriately. Considering the appropriate initial conditions and boundary conditions, the above all create the mathematical model of fluid flow.

3.1 MATERIAL CONSTITUTIVE RELATIONSHIPS AND VISCOSITY MODELS

The relationship between the viscous stress tensor $\boldsymbol{\tau}$ and the rate of strain tensor $\dot{\boldsymbol{\varepsilon}}$ is called a *constitutive equation*. It is the property of material itself and is independent of the special conditions. For different polymers, different constitutive models are used to describe their material properties. Sometimes, because of the need to simplify the problem, different constitutive models would be used for the same type of polymers.

Common constitutive relationships of polymer melt are classified into Newtonian fluids, generalized Newtonian fluids, and viscoelastic fluids.[2,4] In the following section, we introduce these three constitutive relationships and common viscosity models.

3.1.1 Newtonian Fluids

Newton inner friction law is given by

$$\boldsymbol{\tau} = \mu \dot{\boldsymbol{\gamma}} \tag{3.1}$$

where $\boldsymbol{\tau}$ is the shear stress tensor, the velocity gradient is called the *shear rate*; $\dot{\boldsymbol{\gamma}}$ is the rate of strain (or deformation) tensor; and the constant of proportionality μ is called the *viscosity of the fluid*, which is the index of the resistance of fluid to flow.

Fluids for which stress is directly proportional to shear rate, that is Equation 3.1 holds, are called *Newtonian fluids*. For such fluids, the viscosity is usually constant at a given temperature. However, the viscosity may vary with temperature. Fluids for which Equation 3.1 does not hold are called *non-Newtonian fluids*.

The Newtonian fluids include most pure liquids such as water and alcohol, light oil, low molecular weight compounds' solution, and low speed gas. However, molten polymers are non-Newtonian fluids. As its viscosity is

Computer Modeling for Injection Molding: Simulation, Optimization, and Control, First Edition. Edited by Huamin Zhou.

very complicated and nonlinear, it depends on its chemical structure, composition, and processing conditions.

3.1.2 Generalized Newtonian Fluids

In order to model the flow of molten polymers, a modification to Equation 3.1 is made to allow the viscosity to be a function of shear rate. Therefore Equation 3.1 becomes

$$\boldsymbol{\tau} = \eta\left(T, \dot{\boldsymbol{\gamma}}\right)\dot{\boldsymbol{\gamma}} \tag{3.2}$$

where $\boldsymbol{\tau}$ is called the *viscous stress tensor*, which may be written as a matrix of its components:

$$\boldsymbol{\tau} = \begin{bmatrix} \tau_{xx} & \tau_{xy} & \tau_{xz} \\ \tau_{yx} & \tau_{yy} & \tau_{yz} \\ \tau_{zx} & \tau_{zy} & \tau_{zz} \end{bmatrix} \tag{3.3}$$

And $\eta\left(T, \dot{\boldsymbol{\gamma}}\right)$ is called the *viscosity function*, also simply called the *viscosity*.

Most starchy fluids, suspension and plastic melt in the nature are all these kind of fluids. In the case of the non-Newtonian fluids, the viscosity $\eta\left(T, \dot{\boldsymbol{\gamma}}\right)$ decreases when temperature or velocity of flow increases. Furthermore, the plastic materials in molten process are more viscous and compressible.

Generalized Newtonian fluids hold the generalized Newton viscous force law given by

$$\boldsymbol{\sigma} = 2\eta\dot{\boldsymbol{\varepsilon}} - \left(p - \lambda\nabla\cdot\boldsymbol{u}\right)\boldsymbol{I} \tag{3.4}$$

or

$$\boldsymbol{\tau} = 2\eta\dot{\boldsymbol{\varepsilon}} + \left(\lambda\nabla\cdot\boldsymbol{u}\right)\boldsymbol{I} \tag{3.5}$$

where η is the dynamic viscosity, λ is the dilatational viscosity, $\boldsymbol{I}$ is the unit tensor, $\dot{\boldsymbol{\varepsilon}}$ is the rate of strain (or deformation) tensor, and $\boldsymbol{\sigma}$ is the stress tensor, which may always be written in the following form:

$$\boldsymbol{\sigma} = \begin{bmatrix} \sigma_{xx} & \sigma_{xy} & \sigma_{xz} \\ \sigma_{yx} & \sigma_{yy} & \sigma_{yz} \\ \sigma_{zx} & \sigma_{zy} & \sigma_{zz} \end{bmatrix} = -p\boldsymbol{I} + \boldsymbol{\tau} \tag{3.6}$$

For the isotropic fluid, viscous stress is a function of local deformation rate (or strain rate) of fluid. The microunit of the isotropic fluid has nine components of strain rate out of which six components are independent. Rate of strain (or deformation) tensor $\dot{\boldsymbol{\varepsilon}}$ may be written as a matrix of its components:

$$\begin{aligned} \dot{\boldsymbol{\varepsilon}} &= \begin{bmatrix} \dot{\varepsilon}_{xx} & \dot{\varepsilon}_{yx} & \dot{\varepsilon}_{zx} \\ \dot{\varepsilon}_{xy} & \dot{\varepsilon}_{yy} & \dot{\varepsilon}_{zy} \\ \dot{\varepsilon}_{xz} & \dot{\varepsilon}_{yz} & \dot{\varepsilon}_{zz} \end{bmatrix} = \frac{1}{2}\left[\nabla u + (\nabla u)^{\mathrm{T}}\right] \\ &= \begin{bmatrix} \dfrac{\partial u}{\partial x} & \dfrac{1}{2}\left(\dfrac{\partial u}{\partial y} + \dfrac{\partial v}{\partial x}\right) & \dfrac{1}{2}\left(\dfrac{\partial u}{\partial z} + \dfrac{\partial w}{\partial x}\right) \\ \dfrac{1}{2}\left(\dfrac{\partial u}{\partial y} + \dfrac{\partial v}{\partial x}\right) & \dfrac{\partial v}{\partial y} & \dfrac{1}{2}\left(\dfrac{\partial v}{\partial z} + \dfrac{\partial w}{\partial y}\right) \\ \dfrac{1}{2}\left(\dfrac{\partial u}{\partial z} + \dfrac{\partial w}{\partial x}\right) & \dfrac{1}{2}\left(\dfrac{\partial v}{\partial z} + \dfrac{\partial w}{\partial y}\right) & \dfrac{\partial w}{\partial z} \end{bmatrix} \end{aligned} \tag{3.7}$$

And we have

$$\begin{aligned} \dot{\boldsymbol{\gamma}} &= 2\dot{\boldsymbol{\varepsilon}} = \nabla\boldsymbol{u} + (\nabla\boldsymbol{u})^{\mathrm{T}} \\ &= \begin{bmatrix} 2\dfrac{\partial u}{\partial x} & \dfrac{\partial u}{\partial y} + \dfrac{\partial v}{\partial x} & \dfrac{\partial u}{\partial z} + \dfrac{\partial w}{\partial x} \\ \dfrac{\partial u}{\partial y} + \dfrac{\partial v}{\partial x} & 2\dfrac{\partial v}{\partial y} & \dfrac{\partial v}{\partial z} + \dfrac{\partial w}{\partial y} \\ \dfrac{\partial u}{\partial z} + \dfrac{\partial w}{\partial x} & \dfrac{\partial v}{\partial z} + \dfrac{\partial w}{\partial y} & 2\dfrac{\partial w}{\partial z} \end{bmatrix} \end{aligned} \tag{3.8}$$

Thus, Equation 3.5 becomes

$$\boldsymbol{\tau} = \eta\dot{\boldsymbol{\gamma}} + \left(\lambda\nabla\cdot\boldsymbol{u}\right)\boldsymbol{I} \tag{3.9}$$

Notice that $\boldsymbol{\sigma}$, $\dot{\boldsymbol{\varepsilon}}$, and $\boldsymbol{\tau}$ are all symmetric.

In Equation 3.4, $p = -\sigma_{ii}/3$, namely the hydrostatic pressure equals the arithmetic mean of the sum of three normal pressures and its direction is the opposite direction of the normal pressure. To ensure that the relationship is held by the compressible fluid, assume the following equation:

$$\lambda + \frac{2}{3}\mu = 0 \tag{3.10}$$

The fluid satisfying Equation 3.10 also is called *Stokes fluid*.

At present, generalized Newtonian fluid is a widely used constitutive model in the polymer simulation. According to the different practical behavior, the generalized Newtonian fluids can be classified into two categories: time-dependent fluids and time-independent fluids. The former can also be organized into three kinds[4,5]: Bingham plastics, pseudoplastic fluids, and dilatant fluids. The latter can also be further categorized into two kinds: rheopectic fluids and thixotropic fluids.

Bingham plastics are fluids that remain rigid when its shear stress is smaller than yield stress but flow similar to a simple Newtonian fluid once the shear stress has exceeded

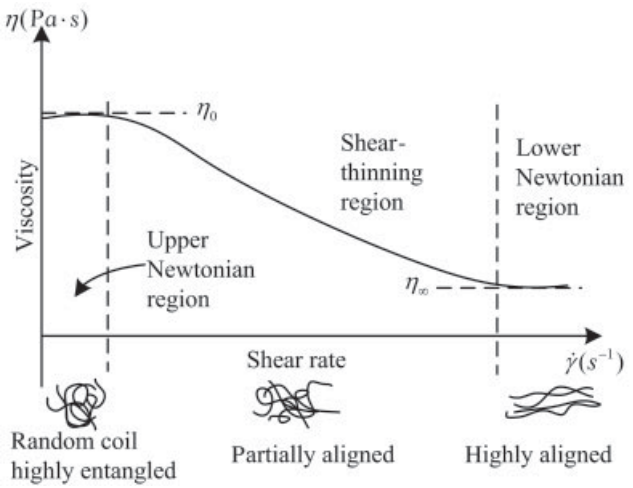

FIGURE 3.1 Characteristic viscosity curve of pseudoplastic fluids.

this value. Different constitutive models representing this type of fluids were developed by Herschel and Bulkley,[6] Oldroyd,[7] and Casson.[8]

Pseudoplastic fluids have no yield stress threshold, and for these fluids, the ratio of shear stress to the rate of shear generally falls continuously and rapidly with increase in the shear rate. Very low and very high shear regions are the exceptions, where the flow curve is almost horizontal (Fig. 3.1). This shear thinning effect that the viscosity decreases with increasing rate of shear stress is an important phenomenon of pseudoplastic fluids. This is currently the most commonly used non-Newtonian viscous fluid model to simulate the polymer flow.

The main characteristic of the dilatant fluids is that at low shear rate, the flow acts basically as a Newtonian fluid; when the shear rate is higher than a certain critical value, viscosity increases with increasing rate of shear (also termed *shear thickening*). Most dilatant fluids are multiphase mixture systems such as asphalt and liquid concrete. The viscosity of time-dependent non-Newtonian fluid has temporal correlation with the constant rate of shear strain. This is less used to describe the polymer melt.

To model the injection molding process, a viscosity function (or model) is required. The viscosity curves of most thermoplastics have the same dependence on shear rates as shown in Figure 3.1. At lower shear rates, the viscosity is nearly a constant. This is the usually called as *upper Newtonian region*. Polymer chains are more uniformly aligned as the shear rate increases, so the viscosity decreases accordingly. This is called the *shear thinning region*. When all polymeric chains are fully aligned, the shear viscosity then becomes virtually insensitive to the shear rate. This is called as *lower Newtonian region*. The upper Newtonian region and shear thinning region can be observed in most polymers (the LCP might be an exception). The lower Newtonian region is, however, not as obvious in most thermoplastics as it occurs with molecular degradation at ultrahigh shear rates.

A number of well-known models are available, so it is important to choose a model that is both accurate over the processing range and for which data can be readily obtained. de Waele in 1923 and Ostwald in 1925 proposed a power law model,[9] also known as Ostwald–de Waele relationship, which can successfully predict the shear thinning region. In 1977, Middleman[10] proposed an advanced power law that overcomes a problem of the original model in which the stress is much higher than that at low rate of shear. The viscosity hardly changes when the rate of shear is very low or very high; namely, at this time, pseudoplastic fluid acts similar to a Newtonian fluid. At least four parameters are required to reflect this relationship between viscosity and shear rate. Cross model[11] and Carreau model[12] are proposed by Cross in 1965 and Carreau in 1972, respectively. All of them are believed to be better than the others in terms of reflecting the characteristics of a thermoplastic polymer. In addition, Sisko model[13] proposed by Sisko in 1958 combined the characteristics of Bingham plastics and power law model. The other models such as Prandtl–Eyring model, Ellis model, Casson model, and fractional exponential model were also applied in some fields successfully. At present, the power law model and the Cross model are widely used in the field of polymer injection molding to describe the viscosity function.[14–21] The following section introduces some common viscosity models.

3.1.2.1 Power Law Model This model has the following form:

$$\eta = \eta_0 \, |\dot{\boldsymbol{\gamma}}|^{n-1} \tag{3.11}$$

$$\eta_0 = B \exp\left(\frac{T_b}{T}\right) \tag{3.12}$$

where η_0 is the Newtonian viscosity or zero-shear rate viscosity, which is defined as the viscosity at zero-shear rate; B is a constant called the *consistency index*; T_b is a constant showing the temperature sensitivity of this material; T is the melting temperature; and n is the power law index with a value between 0 and 1 for polymer melts. When $\eta_0 = \mu$ and $n = 1$, we obtain the relationship for a Newtonian fluid, that is, Equation 3.1. The effective shear rate $|\dot{\boldsymbol{\gamma}}|$ is given by

$$|\dot{\boldsymbol{\gamma}}| = \sqrt{\frac{1}{2}\dot{\gamma}_{ij}\,\dot{\gamma}_{ij}} \tag{3.13}$$

The zero-shear rate viscosity contains the effect of temperature and pressure on viscosity described by some different models. In the field of plastic injection molding process, the WLF model and Arrhenius model are commonly used.

Arrhenius formula is given by

$$\eta_0 = B \exp\left(\frac{T_b}{T}\right) \exp(\beta P) \tag{3.14}$$

where B, T_b, and β are material parameters. This model is suitable for semicrystalline materials.

The WLF zero-shear viscosity model can reflect the variation of melt viscosity with temperature and pressure more exactly. It has the following form:

$$\eta_0 = D_1 \exp\left(\frac{-A_1 (T - (D_2 + D_3 P))}{A_2 + T - D_2}\right) \tag{3.15}$$

in which A_1, A_2, D_1, D_2, and D_3 are material parameters.

Taking natural logarithms of both sides, we obtain

$$\ln(\eta) = (n-1)\ln(\dot{\gamma}) + \ln(\eta_0) \tag{3.16}$$

The above equation shows that this three-parameter model reflects the observation that the viscosity function at medium-high shear rates is nearly a straight line in log–log plots. Therefore, the power law model can represent the behavior of polymer melts in the high shear-rate region. It is also quite easy to fit experimental data with this model and determine the constants η_0 and n.

The main disadvantage of the model is in the low shear-rate range. Despite this disadvantage, the model has been widely used for modeling flow in injection molding. In the filling phase particularly, shear rates are frequently high enough to justify the use of the first-order model.

3.1.2.2 Ellis Model The Ellis model expresses the viscosity as a function of shear stress τ. It has the following form:

$$\frac{\eta_0}{\eta} = 1 + \left(\frac{\tau}{\tau_{1/2}}\right)^{\alpha - 1} \tag{3.17}$$

where $\tau_{1/2}$ is the value of shear stress for which $\eta = \eta_0/2$ and $\alpha - 1$ is the slope of the graph $\ln[(\eta_0/\eta) - 1]$ versus $\ln(\tau/\tau_{1/2})$.

3.1.2.3 Carreau Model The model has the following form:

$$\eta = \eta_\infty + (\eta_0 - \eta_\infty)\left[1 + (K\dot{\gamma})^a\right]^{(n-1)/a} \tag{3.18}$$

where η_∞ is the viscosity at infinite shear rate, η_0 is the viscosity at zero-shear rate, n is a dimensionless constant with the same interpretation as that in Equation 3.11, and K is a material time constant parameter. The Bird–Carreau model is given by $a = 2$. For many shear thinning fluids, $a \approx 2$.

3.1.2.4 Cross Model The equation for the Cross model is given by

$$\eta = \frac{\eta_0}{1 + \left(\frac{\eta_0 |\dot{\boldsymbol{\gamma}}|}{\tau^*}\right)^{1-\tilde{n}}} \tag{3.19}$$

where, τ^* is the shear stress at the transition between Newtonian and power law behavior. If using WLF zero-shear viscosity model presented by Equation 3.15, we call Equation 3.19 as WLF Cross model, which is widely used in injection molding simulation.

3.1.3 Viscoelastic Fluids

Generalized Newtonian fluid model can describe the non-Newtonian characteristic that viscosity changes with the deformation rate tensor. But it cannot predict other phenomena such as recoil, stress relaxation, stress overshoot, and extrudate swell, which are commonly observed in polymer processing flows. These effects have a significant impact on the product quality in polymer processing, and they should not be ignored. The stress of viscoelastic fluid at any time depends on not only the movement and deformation at that moment but also the deformation history. Theoretically, all of these phenomena can be considered as the result of the material that has a combination of the properties of elastic solids and viscous fluids. Therefore, mathematical modeling of polymer processing flows should, ideally, be based on the use of viscoelastic constitutive equations.

In the 1940s, Reiner[22] and Rivlin[23] made a breakthrough in the field of nonlinear viscosity theory and finite elastic deformation theory. The research on the constitute relationship of viscoelastic material had a great development in the following decades. In 1950, Oldroyd[24] first introduced new concepts of coordinate system and derivative going with the material that improved the constitute theory of non-Newtonian fluid to a new level and had been considered as one of important foundations of the constitute theory of modern rheology.

Oldroyd proposed Oldroyd 8-constant model[25] in 1958 in which there is one zero-shear viscosity and seven time constants, and the stress term is kept linear. By letting different constants to be zero, Oldroyd 8-constant model can become Newtonian fluid model, upper-convected Maxwell model (UCM), Oldroyd-B model, second-order model, and Johnson–Segalman model.[26] Among them Oldroyd-B is the most widely used. However, many experiments have also shown that for practical polymer flow, especially for the tensile deformation dominated flow, the results predicted by Oldroyd model and the actual results are quite different.

In 1977, Phan-Thien and Tanner proposed PTT model with 4-constant stress term based on Lodge network theory,[27,28] which can predict both shearing viscosity and

uniaxial extensional viscosity. In 1982, Giesekus proposed 3-constant Giesekus model[29] based on molecular theory, which can predict the normal stress difference besides power law viscosity region of the non-Newtonian fluid. Warner introduced the dumbbell model by abstracting from the dilute polymer solution based on kinematical theory. Referring to this, in 1972, Warner[30] proposed a nonlinear elastic dumbbell model named *FENE* (finitely extensible nonlinear elastic) based on which many scholars improved extended FENE model.[31]

The above-mentioned constitutive equations are all different equations. Integral constitutive relationship applies Boltzmann superposition principle to obtain stress components by accumulation of deformation history with appropriate functions. The simplest integral constitutive model is the one proposed by Lodge[32] for rubberlike liquid in 1964 based on network theory; while the most wildly used model is K-BKZ model proposed by Kaya and Bernstein in 1962, and Kearsley and Zapas[33] in 1963 as independent inventors. K-BKZ model is a nonlinear generalized model, including Rouse–Zimm model, Lodge model, Tanner–Simmons model, and Doi–Edwards model.[26] The constitutive models of integral form can give stress formula explicitly but is not convenient as differential models. In addition, in general condition, they are suitable to be applied in Lagrangian frame, which is a reason why they are not widely used as the differential models.

As the linear models cannot portray well the rheological properties, such as the shear thinning and nonquadratic first normal difference observed in typical melts, it needs to be extended to cover the nonlinear behaviors. The Pom–Pom model proposed by McLeish and Larson[34] in 1998, was considered as a breakthrough in the field of the construction of viscoelastic constitutive equation. It is based on tube theory and a simplified topology of branched molecules. Pom–Pom model still has some disadvantages such as discontinuity phenomena in steady extensional flow, unboundedness of the equation describing the direction in high shearing rate flow, and inexistence of second normal stress difference in shear flow. In 2001, for these shortcomings, Verbeeten et al.[35] proposed an extended Pom–Pom model, namely XPP model. The results of this model are consistent with the results from rheological tests of LDPE. Verbeeten et al.[36,37] adjusted XPP model in 2002 and in 2004 for solving a problem that the principal axis value of tensile stress in radical sign might be negative and kept this method consistent with the other viscoelastic constitutive models in construction. Numerical experiments exhibit that XPP model has some characteristics that the others do not have and can better predict the polymer behaviors in complex flow.[38–40]

The following part will introduce commonly used viscoelasticity models, including upper-convected Maxwell model, Oldroyd-B model, White–Metzner model, Giesekus model, and PTT model.

3.1.3.1 Upper Convected Maxwell Model (UCM) This model describes polymers with linear or quasilinear viscoelasticity, which combines the ideas of viscosity and elasticity. It has the following form:

$$\boldsymbol{\tau} + \lambda_0 \left[\frac{\partial \boldsymbol{\tau}}{\partial t} + (\boldsymbol{u} \cdot \nabla)\, \boldsymbol{\tau} - \nabla \boldsymbol{u}^{\mathrm{T}} \cdot \boldsymbol{\tau} - \boldsymbol{\tau} \cdot \nabla \boldsymbol{u} \right] = \eta \dot{\boldsymbol{\gamma}} \tag{3.20}$$

The relaxation time λ is defined as the time required for stress to be reduced to half of its original value when the polymer stops deforming. A higher relaxation time indicates more memory (elastic) effect.

3.1.3.2 Oldroyd-B Model This model adds an additional Newtonian component to the UCM model as

$$\boldsymbol{\tau}_1 + \lambda_0 \left[\frac{\partial \boldsymbol{\tau}_1}{\partial t} + (\boldsymbol{u} \cdot \nabla)\, \boldsymbol{\tau}_1 - \nabla \boldsymbol{u}^{\mathrm{T}} \cdot \boldsymbol{\tau}_1 - \boldsymbol{\tau}_1 \cdot \nabla \boldsymbol{u} \right] = \eta_1 \dot{\boldsymbol{\gamma}} \tag{3.21}$$

$$\boldsymbol{\tau}_2 = \eta_2 \dot{\boldsymbol{\gamma}} \tag{3.22}$$

$$\boldsymbol{\tau} = \boldsymbol{\tau}_1 + \boldsymbol{\tau}_2 \tag{3.23}$$

$$\eta_2 = r\eta_0, \quad \eta_1 = (1 - r)\, \eta_0 \tag{3.24}$$

If $r = 0$, the model reduces to the UCM model. The model predicts a constant viscosity and a quadratic first normal difference. It should be further noted that linear (or quasilinear) model has been widely used for viscoelastic flow calculations for its simplicity, but it is not suitable for injection molding process because of the lack of shear thinning characteristics. It is suggested to use those models in polymeric solutions for research purpose.

3.1.3.3 White–Metzner Model This model is modified from UCM model. It can illustrate reasonable profiles for shear-rate dependent viscosity h and relaxation time l. It is also easy to select the material parameters on the basis of the first normal stress difference and viscosity. The model is suitable in fast time-dependent motions.

$$\boldsymbol{\tau} + \lambda\,(T, \dot{\boldsymbol{\gamma}}) \left[\frac{\partial \boldsymbol{\tau}}{\partial t} + (\boldsymbol{u} \cdot \nabla)\, \boldsymbol{\tau} - \nabla \boldsymbol{u}^{\mathrm{T}} \cdot \boldsymbol{\tau} - \boldsymbol{\tau} \cdot \nabla \boldsymbol{u} \right] = \eta\,(T, \dot{\boldsymbol{\gamma}})\, \dot{\boldsymbol{\gamma}} \tag{3.25}$$

$$\lambda\,(T, \dot{\boldsymbol{\gamma}}) = \frac{\eta\,(T, \dot{\boldsymbol{\gamma}})}{G} \tag{3.26}$$

Viscosity η and relaxation time λ are both functions of temperature and shear rate. Relaxation time is referenced to the viscosity divided by modulus G.

If λ uses the following form:

$$\lambda\left(T, \dot{\boldsymbol{\gamma}}\right) = \frac{\lambda_0 a_{\mathrm{T}}}{1 + \left(\frac{\lambda_0 a_{\mathrm{T}}}{k}\left|\dot{\boldsymbol{\gamma}}\right|\right)^{1-n}} \tag{3.27}$$

where λ_0 is the relaxation time at zero-shear rate and a_{T} is the shift factor. We call it modified White–Metzner model. The model provides the flexibility by allowing different variation profile for the shear rate and is dependent on the viscosity and relaxation time. The variation of relaxation time is independent on the viscosity and can be fit by cross model.

3.1.3.4 Giesekus Model This model describes the rheological properties with nonlinear stress terms as follows:

$$\boldsymbol{\tau} + \frac{\alpha\lambda_0}{\eta}\boldsymbol{\tau}\cdot\boldsymbol{\tau} + \lambda_0\left[\frac{\partial\boldsymbol{\tau}}{\partial t} + \left(\boldsymbol{u}\cdot\nabla\right)\boldsymbol{\tau} - \nabla\boldsymbol{u}^{\mathrm{T}}\cdot\boldsymbol{\tau} - \boldsymbol{\tau}\cdot\nabla\boldsymbol{u}\right] = \eta_0\dot{\boldsymbol{\gamma}} \tag{3.28}$$

where λ_0 is the relaxation time at zero-shear rate, η_0 is the shear viscosity at zero-shear rate, and α is the dimensionless mobility factor with a value between 0 and 1. The origin of the term involving α can be associated with anisotropic Brownian motion or anisotropic hydrodynamic drag on the constituent polymer molecules. Large decreases in viscosity and normal stress coefficients with increasing shear rate are possible, which is much more realistic than the linear models.

3.1.3.5 PTT Model This model describes the rheological properties with nonlinear stress terms as follows:

$$\left(1 + \frac{\varepsilon\lambda_0}{\eta}tr\left(\boldsymbol{\tau}\right)\right)\boldsymbol{\tau} + \lambda_0\left[\frac{\partial\boldsymbol{\tau}}{\partial t} + \left(\boldsymbol{u}\cdot\nabla\right)\boldsymbol{\tau} - \nabla\boldsymbol{u}^{\mathrm{T}}\cdot\boldsymbol{\tau} - \boldsymbol{\tau}\cdot\nabla\boldsymbol{u}\right] = \eta_0\dot{\boldsymbol{\gamma}} \tag{3.29}$$

where λ_0 is the relaxation time at zero-shear rate, η_0 is the shear viscosity at zero-shear rate, and ε is the material property that controls nonlinear behavior.

The model exhibits shear thinning and nonquadratic first normal stress difference, which is similar in its predictions to the Giesekus equation, except for some minor viscometric features.

3.2 THERMODYNAMIC RELATIONSHIPS

Several thermodynamic properties are required for simulation of injection molding. Thermoplastic generally undergoes a significant volumetric change over temperature and pressure. It is therefore essential to characterize its pressure-volume-temperature (PVT) relationship in order to calculate the compressibility of the material during packing phase and final part's shrinkage and warpage after ejection.

An equation of state relates the three variables, pressure p, specific volume $\hat{V}$, and temperature T. The specific volume is defined as the volume of thermoplastic per unit mass. For any material, we write the state equation in the following form:

$$f\left(p, \hat{V}, T\right) = 0 \tag{3.30}$$

Given any two variables, it is possible to determine the third by using the equation of state. In particular, we can write

$$\hat{V} = g\left(p, T\right) \tag{3.31}$$

where g is some function.

If we graph the PVT data of a material, we would obtain a PVT surface as shown in Figure 3.2. If the material at temperature T_{a} undergoes a change in temperature while being held at constant pressure, the average change in volume over the temperature change is therefore,

$$\frac{\Delta\hat{V}}{\Delta T} = \frac{g\left(p_{\mathrm{a}}, T_{\mathrm{a}} + \Delta T\right) - g\left(p_{\mathrm{a}}, T_{\mathrm{a}}\right)}{\Delta T} = \frac{\hat{V}\left(p_{\mathrm{a}}, T_{\mathrm{a}} + \Delta T\right) - \hat{V}\left(p_{\mathrm{a}}, T_{\mathrm{a}}\right)}{\Delta T} \tag{3.32}$$

In the limit as $\Delta T \to 0$, we obtain the instantaneous change in volume for the material, which we denote by

$$\left(\frac{\partial\hat{V}}{\partial T}\right)_p \tag{3.33}$$

where the subscript p indicates that the pressure is held constant.

The coefficient of volume expansion of the material β is defined as follows:

$$\beta = \frac{1}{\hat{V}}\left(\frac{\partial\hat{V}}{\partial T}\right)_p \tag{3.34}$$

The coefficient of volume expansion is also called the *expansivity of the material*. It has units of reciprocal kelvin (K^{-1}).

Now consider the change in volume because of a change in pressure–temperature constant. This involves moving from point b to c in Figure 3.2. The average change in the volume because of a change in temperature is given by

$$\frac{\Delta\hat{V}}{\Delta T} = \frac{g\left(p_{\mathrm{a}} + \Delta p, T_{\mathrm{b}}\right) - g\left(p_{\mathrm{a}}, T_{\mathrm{b}}\right)}{\Delta p} = \frac{\hat{V}\left(p_{\mathrm{a}} + \Delta p, T_{\mathrm{b}}\right) - \hat{V}\left(p_{\mathrm{a}}, T_{\mathrm{b}}\right)}{\Delta p} \tag{3.35}$$

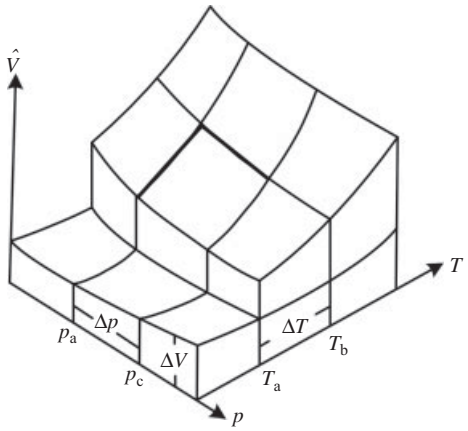

FIGURE 3.2 PVT diagram.

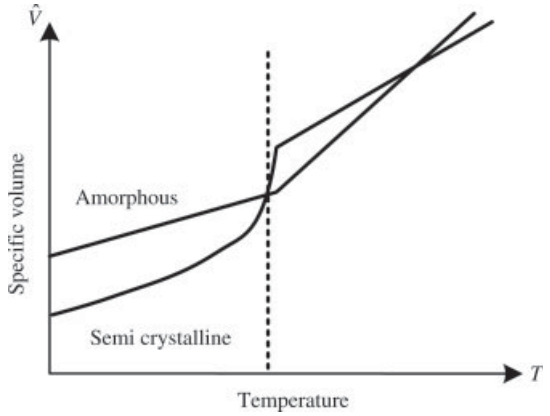

FIGURE 3.3 Specific volume–temperature curves of semicrystalline thermoplastic and amorphous thermoplastic.

Letting $\Delta p \to 0$, we obtain the instantaneous change in volume, which we denote by

$$\left(\frac{\partial \hat{V}}{\partial p}\right)_T \tag{3.36}$$

The isothermal compressibility κ is defined to be

$$\kappa = -\frac{1}{\hat{V}}\left(\frac{\partial \hat{V}}{\partial p}\right)_T \tag{3.37}$$

The negative sign indicates that the volume decreases with increasing pressure. Isothermal compressibility has units of one square meter per newton ($m^2\ N^{-1}$).

Different types of thermoplastic have different PVT behaviors across its transition temperature. Semicrystalline thermoplastic has a significant and abrupt volumetric change, while amorphous thermoplastic has only a change in slope in its specific volume–temperature curves without a sudden transition from melt to solid. Figure 3.3 depicts the difference between these two types of thermoplastics. For semicrystalline materials, the PVT data falls into three areas: low temperature, transition, and high temperature. Figure 2.4 represents the PVT plots of HDPE, a semicrystalline material, and ABS, an amorphous material.

A good PVT model should characterize the dependence of specific volume on temperature and pressure, and the difference between these two types of thermoplastics. There are some PVT models introduced in the following section.

3.2.1 Constant Specific Volume

The constant specific volume model assumes that the specific volume is independent of pressure and temperature. It corresponds to incompressible materials.

This model has the following form:

$$\hat{V} = \hat{V}_0 \tag{3.38}$$

where $\hat{V}$ and $\hat{V}_0$ are the densities of the material. Notice that here $\hat{V}$ represents the density instead of specific volume in this formula. It is intended to be more straightforward. In other PVT models, $\hat{V}$ represents specific volume instead.

3.2.2 Spencer–Gilmore Model

This model is derived from the ideal gas law by adding a pressure and temperature correction term to the specific volume.

This model has the following form:

$$\hat{V} = \hat{V}_0 + \frac{\hat{R}T}{P + P_0} \tag{3.39}$$

where $\hat{V}$ is the specific volume of the material and $\hat{V}_0$ is its reference specific volume at a given condition. There are three parameters to be determined, $\hat{V}_0$, $\hat{R}$, and P_0. T is the material temperature.

3.2.3 Tait Model

The original version of Tait model is

$$\hat{V} = \hat{V}_0\left[1 - C\ln\left(1 + \frac{P}{B}\right)\right] \tag{3.40}$$

$$\hat{V}_0 = b_1 \exp\left(-b_2 T\right) \tag{3.41}$$

$$B = b_3 \exp\left(-b_4 T\right) \tag{3.42}$$

There are five parameters to be determined, b_1, b_2, b_3, b_4, and C. The original version of Tait model cannot deal with the abrupt volumetric change of semicrystalline material.

A modified Tair model can be written in the following form:

$$\hat{V} = \hat{V}_0 \left[1 - C \ln\left(1 + \frac{p}{B}\right)\right] + \hat{V}_t \tag{3.43}$$

$$\hat{V}_0 = \begin{cases} b_{1S} + b_{2S}\bar{T} & \text{if } T \le T_t \\ b_{1L} + b_{2L}\bar{T} & \text{if } T > T_t \end{cases} \tag{3.44}$$

$$B = \begin{cases} b_{3S} \exp\left(-b_{4S}\bar{T}\right) & \text{if } T \le T_t \\ b_{3L} \exp\left(-b_{4L}\bar{T}\right) & \text{if } T > T_t \end{cases} \tag{3.45}$$

$$\hat{V}_t = \begin{cases} b_7 \exp\left(b_8\bar{T} - b_9 p\right) & \text{if } T \le T_t \\ 0 & \text{if } T > T_t \end{cases} \tag{3.46}$$

$$\bar{T} = T - b_5 \tag{3.47}$$

$$T_t = b_5 + b_6 p \tag{3.48}$$

where $C = 0.0894$ and 13 parameters are needed. This model is capable of describing the PVT relationship of both semicrystalline and amorphous materials. Equation 3.46 characterizes the abrupt volumetric change of a semicrystalline material around its melting point. With only linear PVT transitions, b_7, b_8, and b_9 are for amorphous materials. T_t is used to characterize the abrupt viscosity change of the material around its transition temperature.

3.3 THERMAL PROPERTIES MODEL

Thermal properties such as thermal conductivity, specific heat capacity, and thermal diffusivity play critical roles in prediction of heat flow rate, part temperature distribution, and heat and cycle time estimation during filling and packing phases.

According to Fourier's law of unidirectional steady-state heat conduction in an isotropic medium, the thermal conductivity is defined by

$$k = -\frac{\boldsymbol{q}}{\nabla T} \tag{3.49}$$

where $\boldsymbol{q}$ is the heat flux. The thermal diffusivity α determines the transient heat flow and the time-dependent temperature distribution in the polymer. It is related to the thermal conductivity through the following equation:

$$\alpha = \frac{k}{\rho c_p} \tag{3.50}$$

where ρ is the density of the polymer and c_p is the specific heat capacity. In general, thermal diffusivity is determined experimentally from the dynamic temperature response of the polymer.

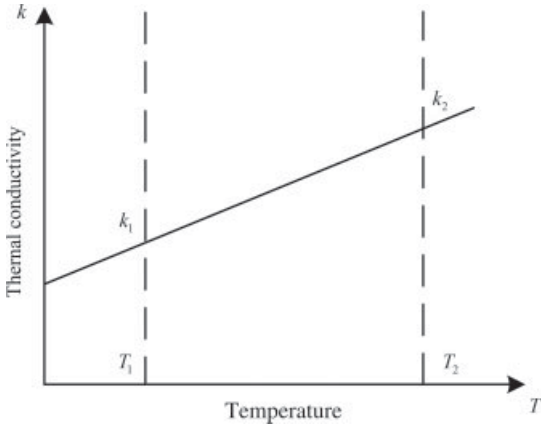

FIGURE 3.4 A schematic diagram of linear interpolation function of thermal conductivity.

Thermal conductivity of thermoplastic appears to be a weak function of temperature, independent of molecular weight, and does not vary significantly from one thermoplastic to the other. The thermal conductivity of thermoplastic is relatively low compared to the mold metal in general. The low thermal conductivity reduces the heat that is transferred to the surroundings. Considering the heat dissipated by viscous forces of high viscosity thermoplastic, the temperature distribution across the thickness of thermoplastic is therefore quite nonisothermal.

The simplest model of the thermal conductivity is the constant thermal conductivity model, namely

$$k = k_0 \tag{3.51}$$

where k is the thermal conductivity and k_0 is its specified value. It assumes that the thermal conductivity is independent of temperature. This model is only supported in most of the commercial simulation software.

The linear interpolation function is another common approximation of the dependence of thermal conductivity on temperature. Given thermal conductivities, k_1 and k_2, at two different temperatures, T_1 and T_2, as shown in Figure 3.4, we can obtain the following linear equation:

$$k = aT + b,\ a = \frac{k_2 - k_1}{T_2 - T_1},\ b = \frac{T_2 k_1 - T_1 k_2}{T_2 - T_1} \tag{3.52}$$

The specific heat capacity is the amount of energy required to heat up a unit mass of the material for 1 °C. If one neglects the effects of possible chemical or physical transformation in the material, the internal energy of the material is related to the material temperature through heat capacity.

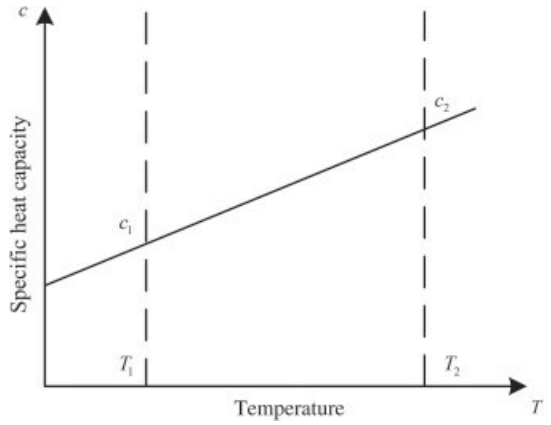

FIGURE 3.5 A schematic diagram of linear interpolation function of specific heat capacity.

Constant specific heat capacity model is generally a good approximation to assume heat capacity to be a constant, namely

$$c_p = c_{p0} \tag{3.53}$$

where c_p is the heat capacity and c_{p0} is a given value. This model is also the only available model in most of the commercial simulation software.

As similar to thermal conductivity, the linear interpolation function is another common approximation of the dependence of heat capacity on temperature. Given thermal conductivities, c_{p1} and c_{p2}, at two different temperatures, T_1 and T_2, we can obtain the following linear equation:

$$c_p = aT + b,\ a = \frac{c_{p2} - c_{p1}}{T_2 - T_1},\ b = \frac{T_2 c_{p1} - T_1 c_{p2}}{T_2 - T_1} \tag{3.54}$$

The schematic diagram of this model is the same as shown in Figure 3.5.

3.4 GOVERNING EQUATIONS FOR FLUID FLOW

The governing equations for fluid flow consist of mass conservation equation, momentum conservation equation, and energy conservation equation. The three equations have the similar form, so a general transport equation can be generalized.

These equations governing the flow of a compressible, viscous fluid are applicable to the flow of a polymer melt and are obtained using the principles of conservation of mass, momentum, and energy. We will derive them briefly.

Consider a material volume of fluid, as shown in Figure 3.6, three measures of coordinate direction in Cartesian coordinate system are δx, δy, and δz. Six surfaces of the microunit are denoted by N, S, E, W, T, and B representing northern, southern, eastern, western, top, and bottom surfaces, respectively. The central point O is on the coordinate (x, y, z).

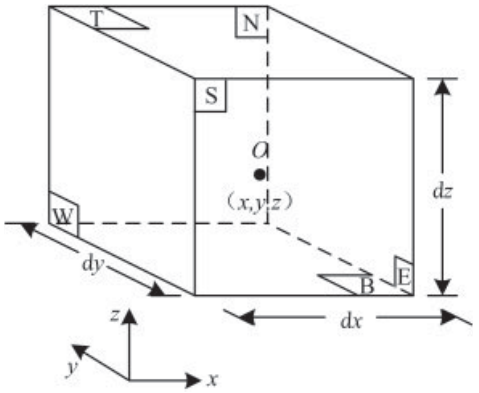

FIGURE 3.6 A material volume of fluid.

All the fluid property parameters are functions of space and time, such as $\rho(x, y, z, t)$, $p(x, y, z, t)$, $T(x, y, z, t)$, and $\boldsymbol{u}(x, y, z)$ representing fluid density, pressure, temperature, and velocity vectors, respectively. The considered material volume of fluid here is small enough that it has enough accuracy to keep the first two terms of Taylor expansion of fluid property parameters on the surfaces. Taking the pressure p, for example, the pressure values on eastern and western surfaces can be represented as

$$p_E = p + \frac{\partial p}{\partial x} \cdot \frac{1}{2}\delta x + o(x) \approx p + \frac{\partial p}{\partial x} \cdot \frac{1}{2}\delta x \tag{3.55}$$

$$p_W = p - \frac{\partial p}{\partial x} \cdot \frac{1}{2}\delta x + o(x) \approx p - \frac{\partial p}{\partial x} \cdot \frac{1}{2}\delta x \tag{3.56}$$

3.4.1 Mass Conservation Equation

If $V(t)$ is the material conservation of mass volume of fluid, in which there are no sources or sinks, then it means that the mass contained in $V(t)$ does not change. That is, the mass increasing rate in the microunit equals net mass inflow flux.

The mass increasing rate in fluid unit is

$$\frac{\partial}{\partial t}(\rho\, \delta x\, \delta y\, \delta z) = \frac{\partial \rho}{\partial t} \cdot \delta x\, \delta y\, \delta z \tag{3.57}$$

The net mass flux through the unit surfaces is the product of density, surface area, and fluid velocity perpendicular to the surfaces. Known from Figure 3.7, the net mass flux through surfaces into fluid unit is

$$\begin{aligned}
&\left[\rho u - \frac{\partial(\rho u)}{\partial x} \cdot \frac{1}{2}\delta x\right]\delta y\, \delta z - \left[\rho u + \frac{\partial(\rho u)}{\partial x} \cdot \frac{1}{2}\delta x\right]\delta y\, \delta z \\
&+ \left[\rho v - \frac{\partial(\rho v)}{\partial y} \cdot \frac{1}{2}\delta y\right]\delta x\, \delta z - \left[\rho v + \frac{\partial(\rho v)}{\partial y} \cdot \frac{1}{2}\delta y\right]\delta x\, \delta z \\
&+ \left[\rho w - \frac{\partial(\rho w)}{\partial z} \cdot \frac{1}{2}\delta z\right]\delta x \delta y - \left[\rho w + \frac{\partial(\rho w)}{\partial z} \cdot \frac{1}{2}\delta z\right]\delta x \delta y
\end{aligned} \tag{3.58}$$

The mass inflow rate is positive, and the outflow one is negative.

Conservation of mass implies that Equation 3.57 equals Equation 3.58, after the simplification, we have

$$\frac{\partial \rho}{\partial t} + \frac{\partial (\rho u)}{\partial x} + \frac{\partial (\rho v)}{\partial y} + \frac{\partial (\rho w)}{\partial z} = 0 \tag{3.59}$$

Writing it in a more compact form:

$$\frac{\partial \rho}{\partial t} + \nabla \cdot (\rho \boldsymbol{u}) = 0 \tag{3.60}$$

where $\boldsymbol{u}$ is the speed vector.

The Equation 3.59 or 3.60 is called the *mass conservation equation* for a compressible fluid, also known as the *continuity equation* or *mass balance equation*.

For an incompressible fluid, the density is constant and so Equation 3.60 becomes

$$\frac{\partial u}{\partial x} + \frac{\partial v}{\partial y} + \frac{\partial w}{\partial z} = 0 \tag{3.61}$$

or

$$\nabla \cdot \boldsymbol{u} = 0 \tag{3.62}$$

Sometimes it is useful to express the continuity equation in terms of the material derivative. Expanding out Equation 3.60, we get

$$\frac{\partial \rho}{\partial t} + \rho (\nabla \cdot \boldsymbol{u}) + \boldsymbol{u} \cdot \nabla \rho = 0 \tag{3.63}$$

Using the chain rule of differentiation, we find that the derivative of the density with respect to time is given by

$$\frac{\mathrm{D}\rho}{\mathrm{D}t} = \frac{\partial \rho}{\partial t} + \frac{\partial \rho}{\partial x}\frac{\partial x}{\partial t} + \frac{\partial \rho}{\partial y}\frac{\partial y}{\partial t} + \frac{\partial \rho}{\partial z}\frac{\partial z}{\partial t} = \frac{\partial \rho}{\partial t} + \boldsymbol{u} \cdot \nabla \rho \tag{3.64}$$

Using Equation 3.64, we may write Equation 3.60 or Equation 3.63 in the following form:

$$\frac{\mathrm{D}\rho}{\mathrm{D}t} = -\rho (\nabla \cdot \boldsymbol{u}) \tag{3.65}$$

3.4.2 Momentum Conservation Equation

Conservation of momentum requires that the time rate of change of fluid particle momentum in a material volume, $V(t)$, be equal to the sum of external forces acting on $V(t)$.

Replace ρ in Equation 3.63 with a characteristic variable φ, representing a certain characteristic parameter per unit mass in fluid microunit, then we obtain the change rate of φ with time per unit mass:

$$\frac{\mathrm{D}\varphi}{\mathrm{D}t} = \frac{\partial \varphi}{\partial t} + \boldsymbol{u} \cdot \nabla \varphi \tag{3.66}$$

And the change rate of φ with time per unit volume in fluid microunit is

$$\rho \frac{\mathrm{D}\varphi}{\mathrm{D}t} = \rho \left(\frac{\partial \varphi}{\partial t} + \boldsymbol{u} \cdot \nabla \varphi \right) \tag{3.67}$$

The two terms on the left side of the equal to sign in Equation 3.60 represent the change rate of fluid mass per unit volume with time and the mass outflow rate per unit volume respectively, namely

$$\frac{\partial \rho}{\partial t} + \nabla \cdot (\rho \boldsymbol{u}) \tag{3.68}$$

Introducing the characteristic variable φ into Equation 3.68, we simply obtain

$$\frac{\partial (\rho \varphi)}{\partial t} + \nabla \cdot (\rho \varphi \boldsymbol{u}) \tag{3.69}$$

which represents the sum of the change rate of φ per unit volume in fluid microunit and net outflow rate of φ per unit volume in fluid microunit. Using the chain rule of differentiation and divergence theorem, Equation 3.69 can be written as

$$\frac{\partial (\rho \varphi)}{\partial t} + \nabla \cdot (\rho \varphi \boldsymbol{u}) = \rho \left(\frac{\partial \varphi}{\partial t} + \boldsymbol{u} \cdot \nabla \varphi \right) + \varphi \left[\frac{\partial \rho}{\partial t} + \nabla \cdot (\rho \boldsymbol{u}) \right] \tag{3.70}$$

Referring to the mass conservation equation, the second term on the right side of the equal to sign in Equation 3.70 equals zero, so we have

$$\rho \frac{\mathrm{D}\varphi}{\mathrm{D}t} = \rho \left(\frac{\partial \varphi}{\partial t} + \boldsymbol{u} \cdot \nabla \varphi \right) = \frac{\partial (\rho \varphi)}{\partial t} + \nabla \cdot (\rho \varphi \boldsymbol{u}) \tag{3.71}$$

The physical meaning of Equation 3.71 is that the increasing rate of φ in Equation 3.71 equals the sum of the increasing rate of φ in fluid microunit and net outflow rate of φ in fluid microunit.

Let φ be the real velocity value to represent momentum change rate of the fluid microunit:

x-component:

$$\varphi = u,\ \rho \frac{\mathrm{D}u}{\mathrm{D}t} = \frac{\partial (\rho u)}{\partial t} + \nabla \cdot (\rho u \boldsymbol{u}) \tag{3.72}$$

y-component:

$$\varphi = v,\ \rho \frac{\mathrm{D}v}{\mathrm{D}t} = \frac{\partial (\rho v)}{\partial t} + \nabla \cdot (\rho v \boldsymbol{u}) \tag{3.73}$$

z-component:

$$\varphi = w,\ \rho \frac{\mathrm{D}w}{\mathrm{D}t} = \frac{\partial (\rho w)}{\partial t} + \nabla \cdot (\rho w \boldsymbol{u}) \tag{3.74}$$

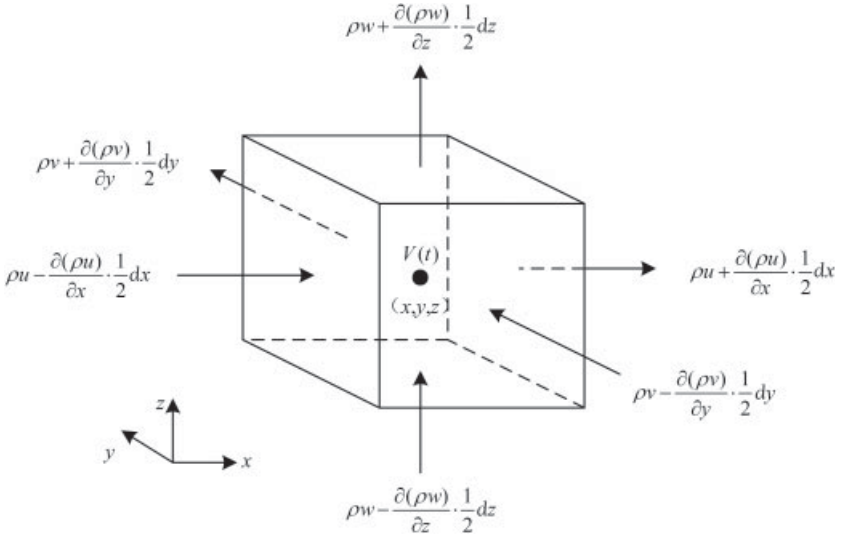

FIGURE 3.7 The mass flux of a fluid microunit.

The combination of the above three equations can be written as

$$\rho\frac{\mathrm{D}\boldsymbol{u}}{\mathrm{D}t}=\frac{\partial(\rho\boldsymbol{u})}{\partial t}+\nabla\cdot(\rho\boldsymbol{u}\boldsymbol{u}) \tag{3.75}$$

The forces on the fluid microunit include surface force and body force. The surface force includes the pressure and viscous force; and body force includes gravity, centrifugal force, electromagnetic force, etc. In general, the surface force is represented as independent stress components; meanwhile, the body force is put into the source term of the equations.

As shown in Figure 3.8, the viscous force components are denoted by τ_{ij}, the subscripts i and j represent the viscous force on the surface perpendicular to i-coordinate direction, whose direction is j-direction. There are nine viscous shear stress components in all, namely, τ_{xx}, τ_{yy}, τ_{zz}, τ_{xy}, τ_{xz}, τ_{yx}, τ_{yz}, τ_{zy}, and τ_{zx}, out of which six components are independent. Referring to equivalent law of shearing stress, we have

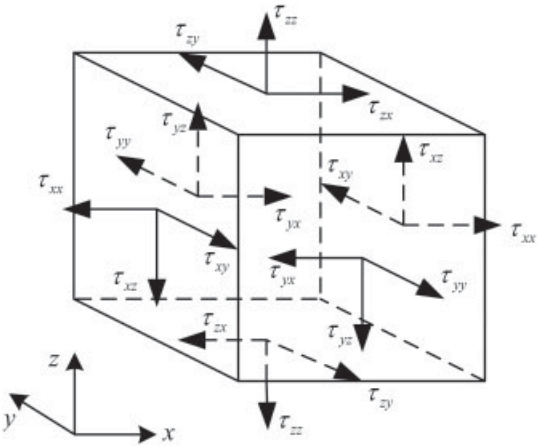

FIGURE 3.8 Surface force components of a fluid microunit.

$$\tau_{xy}=\tau_{yx},\ \tau_{xz}=\tau_{zx},\ \tau_{yz}=\tau_{zy} \tag{3.76}$$

Taking x-direction forces, for example, as shown in Figure 3.8, the forces on the x-direction include the pressure p and the viscous force components τ_{xx}, τ_{yx}, and τ_{zx}. According to Figure 3.7, the resultant forces on the eastern and the western surfaces are

$$\begin{aligned}&\left[\left(p-\frac{\partial p}{\partial x}\cdot\frac{1}{2}\delta x\right)-\left(\tau_{xx}-\frac{\partial\tau_{xx}}{\partial x}\cdot\frac{1}{2}\delta x\right)\right]\delta y\,\delta z\\&\quad+\left[-\left(p+\frac{\partial p}{\partial x}\cdot\frac{1}{2}\delta x\right)+\left(\tau_{xx}+\frac{\partial\tau_{xx}}{\partial x}\cdot\frac{1}{2}\delta x\right)\right]\delta y\,\delta z\\&\quad=\left(-\frac{\partial p}{\partial x}+\frac{\partial\tau_{xx}}{\partial x}\right)\delta x\,\delta y\,\delta z\end{aligned} \tag{3.77}$$

The resultant forces on the southern and the northern surfaces are

$$\begin{aligned}&-\left(\tau_{yx}-\frac{\partial\tau_{yx}}{\partial y}\cdot\frac{1}{2}\delta y\right)\delta z\delta x+\left(\tau_{yx}+\frac{\partial\tau_{yx}}{\partial y}\cdot\frac{1}{2}\delta y\right)\delta z\delta x\\&\quad=\frac{\partial\tau_{yx}}{\partial y}\delta x\delta y\delta z\end{aligned} \tag{3.78}$$

The resultant forces on the top and the bottom surfaces are

$$\begin{aligned}&-\left(\tau_{zx}-\frac{\partial\tau_{zx}}{\partial z}\cdot\frac{1}{2}\delta z\right)\delta x\,\delta y+\left(\tau_{zx}+\frac{\partial\tau_{zx}}{\partial z}\cdot\frac{1}{2}\delta z\right)\delta x\,\delta y\\&\quad=\frac{\partial\tau_{zx}}{\partial z}\delta x\,\delta y\,\delta z\end{aligned} \tag{3.79}$$

Dividing the sum of the above three equations by the volume of the fluid microunit $\delta x\ \delta y\ \delta z$, we obtain the x-direction resultant force of the surfaces on fluid microunit per unit volume:

$$\frac{\partial\left(-p+\tau_{xx}\right)}{\partial x}+\frac{\partial \tau_{yx}}{\partial y}+\frac{\partial \tau_{zx}}{\partial z} \tag{3.80}$$

As mentioned earlier, the body force is denoted as f_x. According to the law of conservation of momentum (also known as *forces balance law*), the momentum conservation equation on the x-direction is

$$\begin{aligned}\rho\frac{\mathrm{D}u}{\mathrm{D}t}&=\frac{\partial(\rho u)}{\partial t}+\nabla\cdot(\rho u\boldsymbol{u})\\&=\frac{\partial\left(-p+\tau_{xx}\right)}{\partial x}+\frac{\partial \tau_{yx}}{\partial y}+\frac{\partial \tau_{zx}}{\partial z}+\rho f_x\end{aligned} \tag{3.81}$$

Similarly, the momentum conservation equations on the y-direction and z-direction:

$$\begin{aligned}\rho\frac{\mathrm{D}v}{\mathrm{D}t}&=\frac{\partial(\rho v)}{\partial t}+\nabla\cdot(\rho v\boldsymbol{u})\\&=\frac{\partial \tau_{xy}}{\partial x}+\frac{\partial\left(-p+\tau_{yy}\right)}{\partial y}+\frac{\partial \tau_{zy}}{\partial z}+\rho f_y\end{aligned} \tag{3.82}$$

$$\begin{aligned}\rho\frac{\mathrm{D}w}{\mathrm{D}t}&=\frac{\partial(\rho w)}{\partial t}+\nabla\cdot(\rho w\boldsymbol{u})\\&=\frac{\partial \tau_{zx}}{\partial x}+\frac{\partial \tau_{zy}}{\partial y}+\frac{\partial\left(-p+\tau_{zz}\right)}{\partial z}+\rho f_z\end{aligned} \tag{3.83}$$

Substituting them into Equation 3.75, we obtain the momentum conservation equation

$$\frac{\partial(\rho\boldsymbol{u})}{\partial t}+\nabla\cdot(\rho\boldsymbol{u}\boldsymbol{u})=\nabla\cdot(\boldsymbol{\sigma})+\rho\boldsymbol{f} \tag{3.84}$$

where $\boldsymbol{\sigma}$ is the stress tensor. For the incompressible case, Equation 3.84 can be written in the following form:

$$\frac{\partial(\rho\boldsymbol{u})}{\partial t}+\rho\boldsymbol{u}\cdot\nabla\boldsymbol{u}=\nabla\cdot(\boldsymbol{\sigma})+\rho\boldsymbol{f} \tag{3.85}$$

If the body force is just the gravity, then

$$f_x=0,\quad f_y=0,\quad f_z=-g \tag{3.86}$$

The viscous stress tensor $\boldsymbol{\tau}$ in Equations 3.84 and 3.85 is unknown.

In order to deal with fluids, it is necessary to have a constitutive relationship between the viscous stress tensor $\boldsymbol{\tau}$ and the rate of strain tensor $\dot{\boldsymbol{\varepsilon}}$. Referring to the earlier introduction, appropriate constitutive equation is selected, and the viscosity model substituted into Equation 3.84 or Equation 3.85 to obtain the corresponding Navier–Stokes equation.

For generalized Newtonian flow, the constitutive equation is Equation 3.4. Thus, the Navier–Stokes equation can be expressed as

$$\begin{aligned}\frac{\partial(\rho u_i)}{\partial t}+\frac{\partial\left(\rho u_i u_j\right)}{\partial x_j}&=-\frac{\partial p}{\partial x_i}+\frac{\partial}{\partial x_j}\left[\mu\left(\frac{\partial u_i}{\partial x_j}+\frac{\partial u_j}{\partial x_i}\right)\right]\\&\quad+\frac{\partial}{\partial x_i}\left(\lambda\frac{\partial u_j}{\partial x_j}\right)+\rho f_i\end{aligned} \tag{3.87}$$

If the fluid is incompressible, we have Equation 3.68, μ is a constant and the dilatational viscosity has no effect. So Equation 3.87 becomes

$$\frac{\partial(\rho u_i)}{\partial t}+\frac{\partial\left(\rho u_i u_j\right)}{\partial x_j}=-\frac{\partial p}{\partial x_i}+\mu\frac{\partial^2 u_i}{\partial x_j^2}+\rho f_i \tag{3.88}$$

or

$$\frac{\partial(\rho\boldsymbol{u})}{\partial t}+\nabla\cdot(\rho\boldsymbol{u}\boldsymbol{u})=-\nabla p+\nabla\cdot(\eta\cdot\nabla\boldsymbol{u})+\rho\boldsymbol{f} \tag{3.89}$$

3.4.3 Energy Conservation Equation

The first law of thermodynamics states that the change rate of total energy in a material volume $V(t)$ is equal to the difference between the work done on the volume and the heat loss of the fluid within the material volume.

Let $E(x,y,z,t)$ denote the total energy of a material volume $V(t)$, then the change rate of E with time per unit mass is

$$\frac{\mathrm{D}E}{\mathrm{D}t}=\frac{\partial E}{\partial t}+\nabla\cdot(E\boldsymbol{u}) \tag{3.90}$$

and the change rate of E with time per unit volume is

$$\rho\frac{\mathrm{D}E}{\mathrm{D}t}=\frac{\partial(\rho E)}{\partial t}+\nabla\cdot(\rho E\boldsymbol{u}) \tag{3.91}$$

Let $\boldsymbol{q}$ denote the heat flux (Fig. 3.9). The rate of heat loss is

x-component:

$$\begin{aligned}&\left[\left(q_x-\frac{\partial q_x}{\partial x}\cdot\frac{1}{2}\mathrm{d}x\right)-\left(q_x+\frac{\partial q_x}{\partial x}\cdot\frac{1}{2}\mathrm{d}x\right)\right]\mathrm{d}y\,\mathrm{d}z\\&\quad=-\frac{\partial q_x}{\partial x}\,\mathrm{d}x\,\mathrm{d}y\,\mathrm{d}z\end{aligned} \tag{3.92}$$

y-component:

$$\begin{aligned}&\left[\left(q_y-\frac{\partial q_y}{\partial y}\cdot\frac{1}{2}\mathrm{d}y\right)-\left(q_y+\frac{\partial q_y}{\partial y}\cdot\frac{1}{2}\mathrm{d}y\right)\right]\mathrm{d}x\,\mathrm{d}z\\&\quad=-\frac{\partial q_y}{\partial y}\,\mathrm{d}x\,\mathrm{d}y\,\mathrm{d}z\end{aligned} \tag{3.93}$$

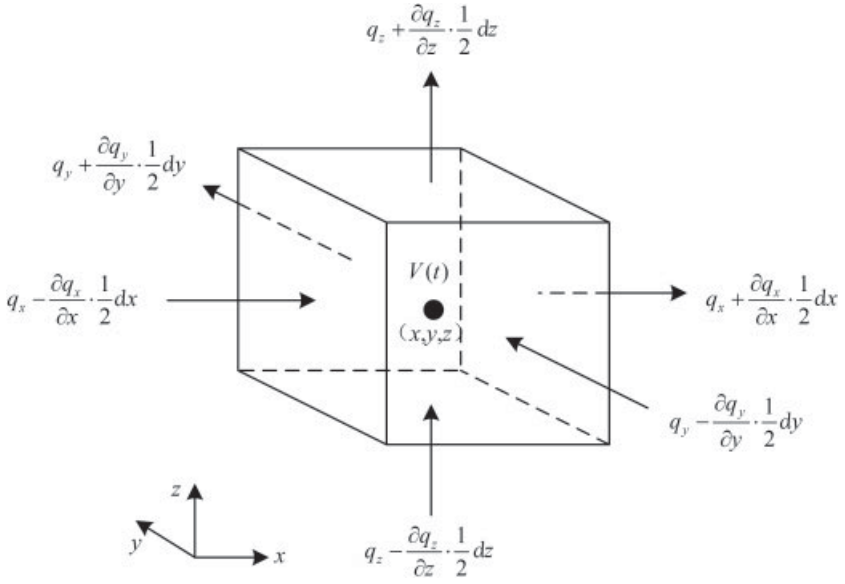

FIGURE 3.9 Heat flux components of a fluid microunit.

z-component:

$$\left[\left(q_z - \frac{\partial q_z}{\partial z} \cdot \frac{1}{2} \mathrm{d}z\right) - \left(q_z - \frac{\partial q_z}{\partial z} \cdot \frac{1}{2} \mathrm{d}z\right)\right] \mathrm{d}x\, \mathrm{d}y = -\frac{\partial q_z}{\partial z} \mathrm{d}x\, \mathrm{d}y\, \mathrm{d}z \tag{3.94}$$

Therefore, the rate of heat loss per unit volume is

$$-\frac{\partial q_x}{\partial x} - \frac{\partial q_y}{\partial y} - \frac{\partial q_z}{\partial z} = -\nabla \cdot \boldsymbol{q} \tag{3.95}$$

According to Fourier heat conduction law, we have

$$\boldsymbol{q} = -k \cdot \nabla T \tag{3.96}$$

where k is the thermal conductivity. So Equation 3.71 becomes

$$-\nabla \cdot \boldsymbol{q} = \nabla \cdot (k \cdot \nabla T) \tag{3.97}$$

The rate of work done on the material volume by external forces is due to both surface and body forces.

The surface forces on x-direction are respected by Equations 3.77–3.79, whose work is

$$\left\{\frac{\partial \left[u\left(-p + \tau_{xx}\right)\right]}{\partial x} + \frac{\partial \left(u\tau_{yx}\right)}{\partial y} + \frac{\partial \left(u\tau_{zx}\right)}{\partial z}\right\} \mathrm{d}x\, \mathrm{d}y\, \mathrm{d}z \tag{3.98}$$

Similarly, the works on y-direction and z-direction are

$$\left\{\frac{\partial \left(v\tau_{xy}\right)}{\partial x} + \frac{\partial \left[v\left(-p + \tau_{yy}\right)\right]}{\partial y} + \frac{\partial \left(v\tau_{zy}\right)}{\partial z}\right\} \mathrm{d}x\, \mathrm{d}y\, \mathrm{d}z \tag{3.99}$$

$$\left\{\frac{\partial \left(w\tau_{zx}\right)}{\partial x} + \frac{\partial \left(w\tau_{zy}\right)}{\partial y} + \frac{\partial \left[w\left(-p + \tau_{zz}\right)\right]}{\partial z}\right\} \mathrm{d}x\, \mathrm{d}y\, \mathrm{d}z \tag{3.100}$$

So, the work of the surface force on the fluid microunit per unit volume is

$$-\nabla \cdot (\rho u) + \left[\frac{\partial \left(u\tau_{xx}\right)}{\partial x} + \frac{\partial \left(u\tau_{yx}\right)}{\partial y} + \frac{\partial \left(u\tau_{zx}\right)}{\partial z} \frac{\partial \left(v\tau_{xy}\right)}{\partial x} + \frac{\partial \left(v\tau_{yy}\right)}{\partial y} + \frac{\partial \left(v\tau_{zy}\right)}{\partial z} + \frac{\partial \left(w\tau_{zx}\right)}{\partial x} + \frac{\partial \left(w\tau_{zy}\right)}{\partial y} + \frac{\partial \left(w\tau_{zz}\right)}{\partial z}\right] \tag{3.101}$$

The total energy of fluid in a material volume is the sum of its kinetic energy e, internal energy i, and geopotential energy, which is always treated as work done by body force such as the gravity.

According to energy conservation law and referring to Equations 3.92, 3.96, and 3.101, we have

$$\frac{\partial (\rho E)}{\partial t} + \nabla \cdot (\rho E \boldsymbol{u}) = -\nabla \cdot (\rho u) + \left[\frac{\partial \left(u\tau_{xx}\right)}{\partial x} + \frac{\partial \left(u\tau_{yx}\right)}{\partial y} + \frac{\partial \left(u\tau_{zx}\right)}{\partial z} + \frac{\partial \left(v\tau_{xy}\right)}{\partial x} + \frac{\partial \left(v\tau_{yy}\right)}{\partial y} + \frac{\partial \left(v\tau_{zy}\right)}{\partial z} + \frac{\partial \left(w\tau_{zx}\right)}{\partial x} + \frac{\partial \left(w\tau_{zy}\right)}{\partial y} + \frac{\partial \left(w\tau_{zz}\right)}{\partial z}\right] + \nabla \cdot (k \cdot \nabla T) + \rho \boldsymbol{u} \cdot \boldsymbol{g} + S_E \tag{3.102}$$

where

$$E = i + e = i + \frac{1}{2}\left(u^2 + v^2 + w^2\right) \tag{3.103}$$

$\rho\, \boldsymbol{gu}$ is the work done by gravity, and S_E is the source term.

We can obtain the expression of change rate of momentum from Equations 3.81–3.83 as

$$\begin{aligned}\frac{\partial(\rho e)}{\partial t} + \nabla\cdot(\rho e\boldsymbol{u}) = -\boldsymbol{u}\cdot\nabla p + u\left(\frac{\partial\tau_{xx}}{\partial x} + \frac{\partial\tau_{yx}}{\partial y} + \frac{\partial\tau_{zx}}{\partial z}\right)\\ + v\left(\frac{\partial\tau_{xy}}{\partial x} + \frac{\partial\tau_{yy}}{\partial y} + \frac{\partial\tau_{zy}}{\partial z}\right)\\ + w\left(\frac{\partial\tau_{zx}}{\partial x} + \frac{\partial\tau_{zy}}{\partial y} + \frac{\partial\tau_{zz}}{\partial z}\right) + \rho\boldsymbol{u}\cdot\boldsymbol{f}\end{aligned} \tag{3.104}$$

Internal energy conservation equation can be obtained by subtracting Equation 3.104 from Equation 3.100:

$$\begin{aligned}\frac{\partial(\rho i)}{\partial t} + \nabla\cdot(\rho i\boldsymbol{u}) = -p\cdot(\nabla\cdot\boldsymbol{u}) + \nabla\cdot(k\cdot\nabla T) + \tau_{xx}\frac{\partial u}{\partial x}\\ + \tau_{yx}\frac{\partial u}{\partial y} + \tau_{zx}\frac{\partial u}{\partial z} + \tau_{xy}\frac{\partial v}{\partial x} + \tau_{yy}\frac{\partial v}{\partial y} + \tau_{zy}\frac{\partial v}{\partial z} + \tau_{zx}\frac{\partial w}{\partial x}\\ + \tau_{zy}\frac{\partial w}{\partial y} + \tau_{zz}\frac{\partial w}{\partial z} + S_i\end{aligned} \tag{3.105}$$

If the fluid is incompressible, then $\nabla\cdot\boldsymbol{u} = 0$, the destiny ρ is a constant, the internal energy $i = cT$ in which c is the specific heat capacity. So Equation 3.105 becomes

$$\begin{aligned}\rho c\frac{\partial T}{\partial t} + c\nabla\cdot(\rho T\boldsymbol{u}) = \nabla\cdot(k\cdot\nabla T) + \tau_{xx}\frac{\partial u}{\partial x} + \tau_{yx}\frac{\partial u}{\partial y}\\ + \tau_{zx}\frac{\partial u}{\partial z} + \tau_{xy}\frac{\partial v}{\partial x} + \tau_{yy}\frac{\partial v}{\partial y} + \tau_{zy}\frac{\partial v}{\partial z}\\ + \tau_{zx}\frac{\partial w}{\partial x} + \tau_{zy}\frac{\partial w}{\partial y} + \tau_{zz}\frac{\partial w}{\partial z} + S_i\end{aligned} \tag{3.106}$$

The specific heat capacity is defined to be the heat capacity per unit mass of material. The unit of specific heat is joules per kilogram per degree kelvin [J/(kg K)]. Specific heat capacity may be measured under conditions of constant volume or pressure and is denoted by c_v or c_p, respectively. Owing to the large stresses exerted on the containing vessel when heating a sample under constant volume, the use of c_p is most common.

If the fluid is incompressible, Equation 3.100 can be represented in the conservation form of enthalpy per unit volume (namely specific enthalpy). Specific enthalpy is defined as

$$h = i + \frac{p}{\rho} \tag{3.107}$$

or total specific enthalpy

$$h_0 = h + \frac{1}{2}\left(u^2 + v^2 + w^2\right) = i + \frac{p}{\rho} + e = E + \frac{p}{\rho} \tag{3.108}$$

The total enthalpy conservation equation can obtained from Equation 3.100

$$\begin{aligned}\frac{\partial(\rho h_0)}{\partial t} + \nabla\cdot(\rho h_0\boldsymbol{u}) = \nabla\cdot(k\cdot\nabla T) + \frac{\partial p}{\partial t}\\ + \left[\frac{\partial(u\tau_{xx})}{\partial x} + \frac{\partial\left(u\tau_{yx}\right)}{\partial y} + \frac{\partial(u\tau_{zx})}{\partial z} + \frac{\partial\left(v\tau_{xy}\right)}{\partial x}\right.\\ + \frac{\partial\left(v\tau_{yy}\right)}{\partial y} + \frac{\partial\left(v\tau_{zy}\right)}{\partial z} + \frac{\partial(w\tau_{zx})}{\partial x}\\ \left. + \frac{\partial\left(w\tau_{zy}\right)}{\partial y} + \frac{\partial(w\tau_{zz})}{\partial z}\right] + \rho\boldsymbol{u}\cdot\boldsymbol{g} + S_\mathrm{h}\end{aligned} \tag{3.109}$$

If it is isotropy generalized Newtonian fluid, referring to constitutive Equations 3.5 and 3.7, Equation 3.105 becomes

$$\frac{\partial(\rho i)}{\partial t} + \nabla\cdot(\rho i\boldsymbol{u}) = -p\cdot(\nabla\cdot\boldsymbol{u}) + \nabla\cdot(k\cdot\nabla T) + \Phi + S_i \tag{3.110}$$

where Φ is the dissipated power:

$$\begin{aligned}\Phi = \mu\left\{2\left[\left(\frac{\partial u}{\partial x}\right)^2 + \left(\frac{\partial v}{\partial y}\right)^2 + \left(\frac{\partial w}{\partial z}\right)^2 + \left(\frac{\partial u}{\partial y} + \frac{\partial v}{\partial x}\right)^2\right.\right.\\ \left.\left. + \left(\frac{\partial u}{\partial z} + \frac{\partial w}{\partial x}\right)^2 + \left(\frac{\partial v}{\partial z} + \frac{\partial w}{\partial y}\right)^2\right]\right\} + \lambda(\nabla\cdot\boldsymbol{u})^2\end{aligned} \tag{3.111}$$

Φ is a nonnegative function representing the effect of all viscous stress; and its physical meaning is the power done by viscous stress (deformation energy) in fluid.

Equations 3.100, 3.105, 3.106, 3.109, and 3.110 are different forms of energy conservation equation.

3.4.4 General Transport Equation

Noticing Equation 3.60, the mass conservation equation, Equation 3.89, the momentum equation, and Equation 3.60, a typical form of energy conservation equation, we will find that although they are equations of different variables, they have a similar form. Let φ denote a general variable (or called *characteristic variable*), then the equations can be written as a unified form:

$$\frac{\partial(\rho\varphi)}{\partial t} + \nabla\cdot(\rho\varphi\boldsymbol{u}) = \nabla\cdot(\Gamma\cdot\nabla\varphi) + S_\varphi \tag{3.112}$$

where Γ is the diffusivity and S_φ is the source term. Equation 3.110 is called *general transport equation*. The

TABLE 3.1 Variables' Selection in General Transport Equation

Equations	φ	Γ	S_φ
Mass conservation equation	1	0	0
x-Component momentum equation	u	η	$-\dfrac{\partial p}{\partial x}+\rho f_x$
y-Component momentum equation	v	η	$-\dfrac{\partial p}{\partial y}+\rho f_y$
z-Component momentum equation	w	η	$-\dfrac{\partial p}{\partial z}+\rho f_z$
Energy conservation equation	i	k	$\Phi+S_i$

first term on left side of equal sign is transient term. The second term is a convection term. The first term on right side of equal to sign is diffusion term. The physical meaning of the equation is that the sum of the change rate of φ with time and the convective outflow rate is equal to the sum of the diffusive increasing rate of φ and the source increasing rate of φ.

Selecting the appropriate choice of φ, Γ, and S_φ, we can obtain the mass conservation equation, the momentum equation, and the energy conservation equation as shown in Table 3.1.

The integral taken over Equation 3.112 on the solution domain and time is

$$\int_t^{t+\Delta t}\int_{\Delta V}\frac{\partial(\rho\varphi)}{\partial t}\mathrm{d}V\,\mathrm{d}t+\int_t^{t+\Delta t}\int_{\Delta V}\nabla\cdot(\rho\varphi\boldsymbol{u})\,\mathrm{d}V\,\mathrm{d}t = \int_t^{t+\Delta t}\int_{\Delta V}\nabla\cdot(\Gamma\cdot\nabla\varphi)\,\mathrm{d}V\,\mathrm{d}t+\int_t^{t+\Delta t}\int_{\Delta V}S_\varphi\,\mathrm{d}V\,\mathrm{d}t \tag{3.113}$$

Using Gauss' Theorem (or the divergence theorem), the above equation becomes

$$\int_t^{t+\Delta t}\int_{\Delta V}\frac{\partial(\rho\varphi)}{\partial t}\mathrm{d}V\,\mathrm{d}t+\int_t^{t+\Delta t}\int_{\Delta S}\boldsymbol{n}\cdot(\rho\varphi\boldsymbol{u})\,\mathrm{d}S\,\mathrm{d}t = \int_t^{t+\Delta t}\int_{\Delta S}\boldsymbol{n}\cdot(\Gamma\cdot\nabla\varphi)\,\mathrm{d}S\,\mathrm{d}t+\int_t^{t+\Delta t}\int_{\Delta V}S_\varphi\mathrm{d}V\,\mathrm{d}t \tag{3.114}$$

in which ΔS is the surface of ΔV and $\boldsymbol{n}$ is the unit outer-normal vector of ΔS. For a steady problem, the transient term is zero, namely

$$\int_t^{t+\Delta t}\int_{\Delta S}\boldsymbol{n}\cdot(\rho\varphi\boldsymbol{u})\,\mathrm{d}S\,\mathrm{d}t=\int_t^{t+\Delta t}\int_{\Delta S}\boldsymbol{n}\cdot(\Gamma\cdot\nabla\varphi)\,\mathrm{d}S\,\mathrm{d}t+\int_t^{t+\Delta t}\int_{\Delta V}S_\varphi\,\mathrm{d}V\,\mathrm{d}t \tag{3.115}$$

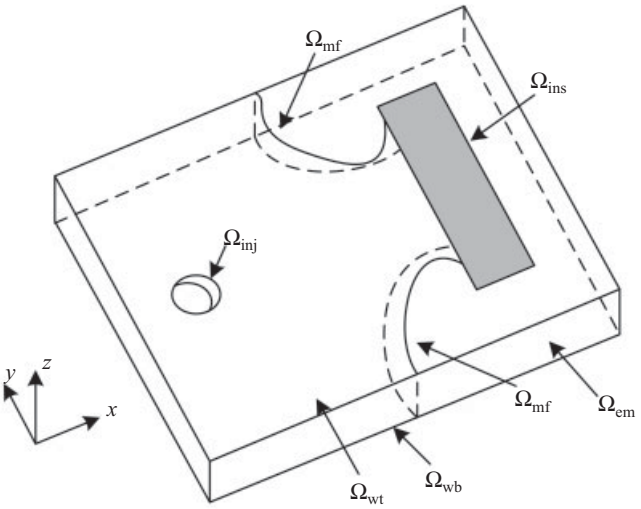

FIGURE 3.10 Boundary conditions for injection molding simulation.

3.5 BOUNDARY CONDITIONS

After obtaining the governing equations, we consider boundary conditions for the problem of injection molding. Unlike the governing equations, boundary conditions are quite specific for a particular problem. Therefore, it is possible to describe boundary conditions for our problem, which will hold for both the general equations and the simplified equations for injection molding.

Figure 3.10 illustrates a simple mold cavity for which we discuss the required boundary conditions. There are several surfaces on which boundary conditions need be described:

- Ω_{inj} is the surface through which the melt is injected into the cavity.
- Ω_{em} is the surface defining the edge of the mold, which is in contact with the melt.
- Ω_{wt} and Ω_{wb} is the top and bottom surface of the mold wall, respectively.
- Ω_{ins} is the surface defining any insert in the mold. It is possible to have any number in a real cavity.
- Ω_{mf} is the surface defining the position of the melt front.

For the injection molding problem, boundary conditions relate to the solution of the pressure and thermal distributions in the cavity. In fact, it is possible to combine the continuity and momentum equations into a single equation for pressure. This pressure equation is coupled to the energy equation because the material's viscosity, which affects pressure, is determined by both the temperature and shear rate. Solution to the injection molding problem therefore

requires solution to the pressure and energy equations. The pressure and thermal boundary conditions will be discussed separately in the following section.

3.5.1 Pressure Boundary Conditions

The boundary conditions relating to pressure are as follows:

- At any impermeable boundary, the pressure gradient in the normal direction to the boundary is zero. The impermeable boundaries are the mold edges, the mold walls, and any mold inserts. Therefore, we have

$$\frac{\partial p}{\partial n} = 0 \text{ on } \Omega_{\text{em}}, \Omega_{\text{wt}}, \Omega_{\text{wb}}, \quad \text{and} \quad \Omega_{\text{ins}} \tag{3.116}$$

Physically, this means that it cannot flow through the mold walls or edges.

- The melt flow rate q, which can determine the gate speed, or the pressure p, is specified at the surface where the melt enters the cavity (also known as *gate*). That is,

$$q = q_{\text{inj}} \text{ or } p = p_{inj} \text{ on } \Omega_{\text{inj}} \tag{3.117}$$

Engineers usually use a specified flow rate in the filling phase. This is obtained by dividing the volume of the part to be molded by the user-specified fill time. It is possible to vary this flow rate to model injection profiling. For the packing phase, it is common to specify a pressure at the points of injection gate. So, this may also vary from model packing profiles.

- Assuming that the pressure datum is atmospheric pressure, the pressure is zero at the melt front. That is,

$$p = 0 \text{ on } \Omega_{\text{mf}} \tag{3.118}$$

As most molds are vented that allow air ahead of the melt to escape, this is physically sensible.

3.5.2 Temperature Boundary Conditions

The boundary conditions relating to temperature are as follows:

- The temperature profile through the cavity thickness, $T(z)$, is prescribed for the surface through which the melt is injected. That is

$$T(z) = T_{\text{inj}}(z) \tag{3.119}$$

Most flow analysis software assumes that the melt temperature is uniform at the point of injection. In practice, this is not too critical because the melt is rapidly convected into the cavity or runner system, where thermal effects allow a temperature profile across the thickness to develop quickly because of shear heating and conduction.

- The temperature, T, is prescribed on all mold boundaries. A different temperature can be prescribed on each boundary. That is,

$$T = T_{\text{em}} \text{ on } \Omega_{\text{em}} \tag{3.120}$$

$$T = T_{\text{wt}} \text{ on } \Omega_{\text{wt}} \tag{3.121}$$

$$T = T_{\text{wb}} \text{ on } \Omega_{\text{wb}} \tag{3.122}$$

$$T = T_{\text{ins}} \text{ on } \Omega_{\text{ins}} \tag{3.123}$$

Recently, it has become common to first perform a thermal analysis of the mold and its cooling system, and then use the results from this analysis to define the temperatures on the mold for flow analysis.

3.5.3 Slip Boundary Condition

At fluid–solid boundaries, the impermeable condition has been widely accepted, namely the melt has zero on the normal direction of the wall. This can be expressed as

$$\boldsymbol{u} \cdot \boldsymbol{n} = 0 \text{ on } \Omega_{\text{em}}, \ \Omega_{\text{wt}}, \text{ and } \Omega_{\text{wb}} \tag{3.124}$$

where $\boldsymbol{n}$ is the normal vector of mold wall and edge.

While for the tangential direction of wall, the no-slip condition[41,42] is commonly used as

$$\boldsymbol{u} \cdot \boldsymbol{t} = 0 \text{ on } \Omega_{\text{em}}, \ \Omega_{\text{wt}}, \text{ and } \Omega_{\text{wb}} \tag{3.125}$$

where $\boldsymbol{t}$ is the tangential vector of the wall. It is based on the following assumption: the shear stress on the interface is always less than the critical value required by the liquid to wet the solid wall. So the liquid adhesive to the wall moves (or keeps static) with the same velocity of the wall together.

From Equations 3.124 and 3.125, we have

$$\boldsymbol{u} = 0 \text{ on } \Omega_{\text{em}}, \ \Omega_{\text{wt}}, \text{ and } \Omega_{\text{wb}} \tag{3.126}$$

As with most engineering approximations, the no-slip condition does not always hold in reality. Many scholars considered that in the polymer molding process, the shear stress on the cavity surface is always bigger than the critical value, as a result of which the fluid would slip on the cavity wall instead of being adhesive with it.[43] On the other hand, the no-slip condition will cause stress singularity on the contact line, especially for the free surface tracing methods with free surface different equation. For the tracing methods with particles or volume function, the problem that stress changes tempestuously at contact points still exists, although it is not so bad as the former, which is difficult to treat in numerical simulation. If using

nonslip condition, the stress singularity on the contact line is basically eliminated because the velocity near the contact line changes continuously.[44–46]

Hockin[45] considered that the melt on the cavity wall is slipable and is effected by the friction. The friction depends on slip coefficient and the tangential velocity of the fluid on the cavity wall. Silliman and Scriven[47] proposed the Navier slip condition according to the Navier linear–slip length model[48] and established a quantitative relationship between the slip velocity and the shear stress of the wall shown as

$$[\beta \boldsymbol{\tau} \cdot \boldsymbol{n} + (\boldsymbol{u} - \boldsymbol{u}_{\mathrm{b}})] \cdot \boldsymbol{t}^{\mathrm{T}} = 0 \tag{3.127}$$

in which $\boldsymbol{t}$ and $\boldsymbol{n}$ represent the tangential and outer-normal unit vectors at boundaries, respectively, $\boldsymbol{\tau}$ is the deviatoric stress tensor or viscous stress tensor, β is slip coefficient, and $\boldsymbol{u}$ and $\boldsymbol{u}_{\mathrm{b}}$ are the velocity of the fluid particle and the cavity wall.

We can obtain the relationship between external force on the fluid at slip boundaries and the velocity of the fluid from Equation 3.127. In general case, the velocity of the cavity wall is zero, so the relationship can be written in the following form:

$$T_{\mathrm{f}} = -\frac{u_{\mathrm{t}}}{\beta} \tag{3.128}$$

in which T_{f} is the tangential external force on the fluid and u_{t} is the tangential component of the fluid velocity on the cavity wall.

Besides the linear–slip length model represented by Equation 3.127, the common slip boundary models include ultimate shear stress–slip model[49,50] and nonlinear–slip length model.[51,52] In linear–slip length model, it is considered that the slip occurs just when the shear stress exists at the fluid–solid interface and the slip coefficient (often represented by the slip length) is a constant. The ultimate shear stress–slip model considers that no slip occurs at low shear rate (or shear stress); the slip would occur only when shear rate (or shear stress) reaches an ultimate value. The nonlinear–slip length model considers that the slip coefficient is a constant at low shear rate, so it becomes linear–slip length model; while at high shear rate, the slip coefficient and the shear rate shows a strong nonlinear relationship, which can be described by the ultimate shear stress–slip model. The last two models are relatively complex and have some difficulties in theoretical analysis and numerical calculation. They are applied in research on micro–nano scale flow.

3.6 MODEL SIMPLIFICATIONS

The equations of governing the behavior of a fluid motion were derived in the preceding section of this chapter. They are the continuity, momentum, and energy equations shown as

$$\frac{\partial \rho}{\partial t} + \nabla \cdot (\rho \boldsymbol{u}) = 0 \tag{3.129}$$

$$\frac{\partial (\rho \boldsymbol{u})}{\partial t} + \nabla \cdot (\rho \boldsymbol{u}\boldsymbol{u}) = \nabla \cdot (\boldsymbol{\sigma}) + \rho \boldsymbol{f} \tag{3.130}$$

$$\begin{aligned} \rho c \frac{\partial T}{\partial t} + c\nabla \cdot (\rho T \boldsymbol{u}) = {} & \nabla \cdot (k \cdot \nabla T) + \tau_{xx} \frac{\partial u}{\partial x} + \tau_{yx} \frac{\partial u}{\partial y} \\ & + \tau_{zx} \frac{\partial u}{\partial z} + \tau_{xy} \frac{\partial v}{\partial x} + \tau_{yy} \frac{\partial v}{\partial y} + \tau_{zy} \frac{\partial v}{\partial z} + \tau_{zx} \frac{\partial w}{\partial x} \\ & + \tau_{zy} \frac{\partial w}{\partial y} + \tau_{zz} \frac{\partial w}{\partial z} + S_i \end{aligned} \tag{3.131}$$

These equations are quite general and hold for all common fluids. With today's computer hardware and numerical techniques, it is not feasible to solve them in complicated domains such as injection mold cavities. Our application is injection molding, and it is possible to simplify the equations for this purpose.

Injection molding is a cyclic process with three fundamental steps: filling phase, packing phase, and cooling phase. In the filling stage, a polymer melt is injected into the cold-walled cavity, where it spreads under the action of high pressures and fills the mould. In the packing stage, after the mould is filled, high pressure is maintained, and additional melt flows into the cavity to compensate for density changes (shrinkage) during cooling. And in the last step, the melt is cooled, and the shaped article is ejected. We focus on different fluid characteristics during the filling and packing phases, so the assumptions, boundary conditions and further simplified numerical models are different in the simulation of these two phases.

To make solution times and material data requirements more reasonable, a number of assumptions are made. In the following section, we discuss these assumptions and produce a simplified set of equations for analysis of the filling and packing phases, respectively.

3.6.1 Hele–Shaw Model

At present, the most widely used model simplification in polymer processing simulation is the Hele–Shaw model (named after Henry Selby Hele–Shaw). It applies to flows in small gap. Conventionally, most of plastic products have thin shell structures. The thickness of most plastic products is far beyond the planar directions, such that $\frac{h}{L} \ll 1$ and $\frac{h}{W} \ll 1$, and the gap vary slowly such that $\frac{\partial h}{\partial x} \ll 1$ and $\frac{\partial h}{\partial y} \ll 1$. In addition, the long molecular chain structure causes a high viscosity, so the inertia force is much smaller than viscous shear stress. So the filling flow in a thin cavity can be approximated to Hele–Shaw flows. Figure 3.11

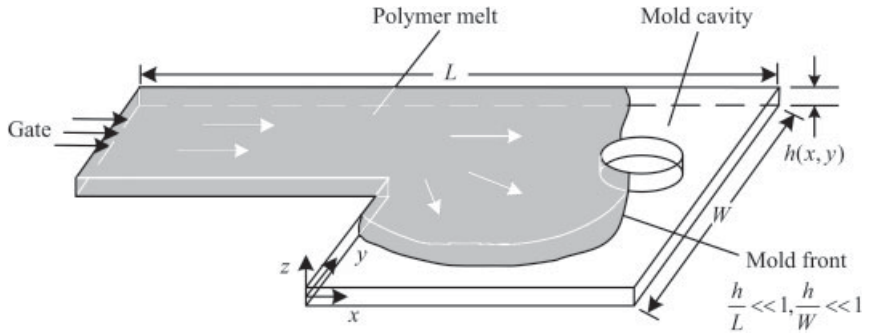

FIGURE 3.11 A schematic diagram of a typical flow described by the Hele–Shaw model.

represents a typical flow described by the Hele–Shaw model.

The governing equation of Hele–Shaw flows is identical to that of the inviscid potential flow and to the flow of fluid through a porous medium (Darcy's law). It thus permits visualization of this kind of flow in two dimensions.

Hele–Shaw approximation believes the following assumptions:

1. The filling flow of melt can be considered as extended laminar flow of incompressible fluid. The velocity in the thickness direction can be ignored and the pressure keeps constant.
2. Because of the high viscosity, the inertial force that is much smaller than viscous shear stress can be ignored.
3. Ignore the heat convection in the thickness direction.
4. In the direction of melt flow, heat conduction is slightly relative to heat convection, hence it can be ignored.
5. Do not consider the cross flow at the melt flow front, namely fountain effect.
6. Ignore the effect of gap on simulation.

The Hele–Shaw approximation (Shell model) is a good tool to simulate the thin parts injection molding processing. To model a solid part with thin shell structure, the geometry of the solid part is simplified into mid-plane model or the surface model.

3.6.2 Governing Equations for the Filling Phase

- During the filling phase, the melt is assumed to be incompressible.

This assumption means that the density is constant and the dilatational viscosity $\lambda = 0$. So Equation 3.127 becomes

$$\nabla \cdot \boldsymbol{u} = 0 \tag{3.132}$$

And by substituting Equation 3.130 in Equation 3.131, we have

$$\begin{aligned} \nabla \cdot (\rho \boldsymbol{u}\boldsymbol{u}) &= \rho (\nabla \cdot \boldsymbol{u}\boldsymbol{u}) = \rho \boldsymbol{u} (\nabla \cdot \boldsymbol{u}) + \rho (\boldsymbol{u} \cdot \nabla \boldsymbol{u}) \\ &= \rho (\boldsymbol{u} \cdot \nabla \boldsymbol{u}) \end{aligned} \tag{3.133}$$

- During the filling phase, the melt can be represented as a Generalized Newtonian Fluid. This assumption implies that viscoelastic effects will be ignored, and we can use the constitutive relationship and viscosity models for the generalized Newtonian fluid. And because of the earlier assumption that the melt is incompressible, the deviatoric strain tensor and the strain rate tensor are equal.

Using Equations 3.2, 3.6, and 3.8, we have

$$\begin{aligned} \nabla \cdot (\boldsymbol{\sigma}) &= \nabla \cdot (-p\boldsymbol{I} + \eta \dot{\boldsymbol{\gamma}}) = -\nabla p + \nabla \cdot \eta \dot{\boldsymbol{\gamma}} \\ &= -\nabla p + \nabla \cdot \eta \left(\nabla \boldsymbol{u} + \nabla \boldsymbol{u}^{\mathrm{T}}\right) \end{aligned} \tag{3.134}$$

And Equation 3.131 becomes Equation 3.110.

- During the filling phase, the thermal conductivity of the material is assumed to be constant. Despite the fact that the thermal conductivity k of polymers depends on temperature, this assumption is enforced because of the difficulty in obtaining material data.

Using the assumption the term involving k in Equation 3.131 becomes

$$\nabla \cdot (k \cdot \nabla T) = k \nabla \cdot \nabla T = k \nabla^2 T \tag{3.135}$$

Enforcing the assumptions above gives the following equations:

$$\nabla \cdot \boldsymbol{u} = 0 \tag{3.136}$$

$$\frac{\partial (\rho \boldsymbol{u})}{\partial t} + \rho (\boldsymbol{u} \cdot \nabla \boldsymbol{u}) = -\nabla p + \nabla \cdot \eta \left(\nabla \boldsymbol{u} + \nabla \boldsymbol{u}^{\mathrm{T}}\right) + \rho \boldsymbol{f} \tag{3.137}$$

$$\frac{\partial (\rho i)}{\partial t} + \nabla \cdot (\rho i \boldsymbol{u}) = k \nabla^2 T + \Phi + S_i \tag{3.138}$$

3.6.3 Governing Equations for the Packing Phase

During the packing phase, it is essential to consider the effect of melt compressibility. Therefore, the relation $\nabla \cdot \boldsymbol{u} = 0$ may not be used to simplify the equations. We do, however, use all the other assumptions regarding material behavior and geometry as discussed in the previous section.

The continuity equation in the packing phase is

$$\frac{\partial \rho}{\partial t} + \nabla \cdot (\rho \boldsymbol{u}) = 0 \tag{3.139}$$

We know the term $\nabla \cdot (\rho \boldsymbol{u}\boldsymbol{u})$ in the momentum equation can be expanded as follows:

$$\nabla \cdot (\rho \boldsymbol{u}\boldsymbol{u}) = \rho (\boldsymbol{u} \cdot \nabla \boldsymbol{u}) + (\nabla \cdot \rho \boldsymbol{u}) \boldsymbol{u} \tag{3.140}$$

And

$$\frac{\partial}{\partial t} (\rho \boldsymbol{u}) = \frac{\partial \rho}{\partial t} \boldsymbol{u} + \rho \frac{\partial \boldsymbol{u}}{\partial t} = - (\nabla \cdot \rho \boldsymbol{u}) \boldsymbol{u} + \rho \frac{\partial \boldsymbol{u}}{\partial t} \tag{3.141}$$

We obtain

$$\frac{\partial}{\partial t} (\rho \boldsymbol{u}) = \rho (\boldsymbol{u} \cdot \nabla \boldsymbol{u}) - \nabla \cdot \rho \boldsymbol{u}\boldsymbol{u} + \rho \frac{\partial \boldsymbol{u}}{\partial t} \tag{3.142}$$

Substituting the above equations in the momentum equation, we have

$$\rho \frac{\partial \boldsymbol{u}}{\partial t} = -\rho (\boldsymbol{u} \cdot \nabla \boldsymbol{u}) + \nabla \cdot \boldsymbol{\sigma} + \rho \boldsymbol{f} \tag{3.143}$$

Using the assumption that the melt be considered as a generalized Newtonian fluid, Equation 3.142 becomes

$$\rho \frac{\partial \boldsymbol{u}}{\partial t} = -\nabla p - \rho (\boldsymbol{u} \cdot \nabla \boldsymbol{u}) + \nabla \cdot \eta \dot{\boldsymbol{\gamma}} + \rho \boldsymbol{f} \tag{3.144}$$

We use the same assumptions in the packing phase as that used in the filling phase except that the fluid is considered compressible now. The energy equation becomes

$$\rho c_{\mathrm{p}} \left(\frac{\partial T}{\partial t} + \boldsymbol{u} \cdot \nabla T \right) = \beta T \left(\frac{\partial p}{\partial t} + \boldsymbol{u} \cdot \nabla p \right) + \eta \dot{\boldsymbol{\gamma}} + k \nabla^2 T \tag{3.145}$$

Equations 3.139, 3.144, and 3.145 are the continuity, momentum, and energy equations, respectively, governing the behavior of a fluid motion during the packing phase.

REFERENCES

1. Fung Y.C., A First Course in Continuum Mechanics. 1977, New York: Prentice-Hall.
2. Tanner R.I., Engineering Rheology. 1985, Oxford: Clarendon.
3. Liu I-S., Continuum Mechanics. 2002, Berlin: Springer.
4. Nassehi V., Pactical Aspects of Finite Element Molding of Polymer Processing. 2002, Chichester: John Wiley & Sons.
5. Lenk R.S., Polymer Rheology. 1978, London: Kluwer Academic Pub.
6. Herschel W.H., Bulkley R., Flow of non-Newtonian fluids, in Encyclopedia of Fluid Mechanics. Rudraiah K.P.N., Editors. 1927, Gulf: Houston.
7. Oldroyd J.G., A Rational Formulation of the Equations of Plastic Flow for a Bingham Solid, in Proceedings of the Cambridge Philosophical Society. 1947, Cambridge: Cambridge Univ Press. 100–105.
8. Casson N., Rheology of Disperse Systems. Mill C.C., Editor 1959, London: Pergamon.
9. Bird R.B., Armstrong R.C., Hassager O., Dynamics of polymeric liquids, Vol. 1. Fluid Mechanics. 1987, New York: John Wiley and Sons Inc.
10. Middleman S., Greener J., Malone M., Fundamentals of Polymer Processing. 1977, New York: McGraw-Hill.
11. Cross M.M., Rheology of non-newtonian fluids: a new flow equation for pseudoplastic systems. Journal of Colloid Science, 1965. **20**(5): 417–437.
12. Carreau P.J., Rheological equations from molecular network theories. Journal of Rheology, 1972. **16**(1): 99–127.
13. Sisko A.W., The flow of lubricating greases. Industrial & Engineering Chemistry, 1958. **50**(12): 1789–1792.
14. Liu C.T., Chen J.B., Wang L.X., et al., Numerical analysis of injection mold filling process. Mechanics and Engineering, 1999. **21**(2): 37–39.
15. Cao W., Wang R., Shen C.Y., 3D melt flow simulation in injection molding. Journal of Chemical Industry and Engineering (China), 2009. **55**(9): 1493–1498.
16. Geng T., Li D.Q., Zhou H.M., Numerical simulation of filling stage in injection molding based on a 3D model. China Plastics, 2003. **17**(7): 78–81.
17. Chen J.L., The numerical simulation and application of the flow behaviour of the polymer in the injection process. Die and Mould Technology, 1997. (3): 29–33.
18. Wang L.X., Liu C.T., Shen C.Y., et al., Dynamic simulation of injection mould filling process. China Plastics, 1996. **10**(5): 71–77.
19. Ma D.J., Chen J.N., Simulations of three-dimensional flow fields in metering section of screw during plasticization process. Journal of Petrochemical Universities, 2006. **19**(2): 76–79.
20. Sun Y.P., Liu H.S., Xiong H.H., et al., Numerical simulation of gas assisted injection molding process. Plastics Science and Technology, 2000. (5): 38–40.
21. Lin L.F., Pen Y.S., Application of finite-element method to the solution of pressure field of filling in injection molding. Journal of Zhejiang University (Engineering Science), 2000. **34**(1): 9–14.
22. Reiner M., A mathematical theory of dilatancy. American Journal of Mathematics, 1945. **67**(3): 350–362.
23. Rivlin R.S., The hydrodynamics of non-Newtonian fluids. I. Proceedings of the Royal Society A, 1948. **193**(1033): 260–281.

24. Oldroyd J.G., On the formulation of rheological equations of state. Proceedings of the Royal Society of London. Series A, Mathematical and Physical Sciences. 1950, JSTOR: 523–541.
25. Oldroyd J.G., Non-Newtonian effects in steady motion of some idealized elastic-viscous fluids. Proceedings of the Royal Society of London. Series A, Mathematical and Physical Sciences, 1958. **245**: 278–297.
26. Bird R.B., Wiest J.M., Constitutive equations for polymeric liquids. Annual Review of Fluid Mechanics, 1995. **27**(1): 169–193.
27. Thien N.P., Tanner R.I., A new constitutive equation derived from network theory. Journal of Non-Newtonian fluid mechanics, 1977. **2**(4): 353–365.
28. Phan-Thien N., A nonlinear network viscoelastic model. Journal of Rheology, 1978. **22**: 259–283.
29. Giesekus H., A simple constitutive equation for polymer fluids based on the concept of deformation-dependent tensorial mobility. Journal of Non-Newtonian fluid mechanics, 1982. **11**(1–2): 69–109.
30. Warner H.R., Kinetic theory and rheology of dilute suspensions of finitely extensible dumbbells. Industrial and Engineering Chemistry Fundamentals, 1972. **11**: 379–387.
31. Herrchen M., Ottinger H.C., A detailed comparison of various FENE dumbbell models. Journal of Non-Newtonian Fluid Mechanics, 1997. **68**(1): 17–42.
32. Lodge A.S., Elastic Liquids. 1964, London: Academic Press.
33. Bernstein B., Kearsley E.A., Zapas L.J., A study of stress relaxation with finite strain. Journal of Rheology, 1963. **7**(1): 391–410.
34. McLeish T.C.B, Larson R.G., Molecular constitutive equations for a class of branched polymers: The pom-pom polymer. Journal of rheology, 1998. **42**: 81–110.
35. Verbeeten W.M.H., Peters G.W.M., Baaijens F.P.T., Differential constitutive equations for polymer melts: the eXtended Pom–Pom model. Journal of rheology, 2001. **45**(4): 823–843.
36. Verbeeten W.M.H., Peters G.W.M., Baaijens F., Viscoelastic analysis of complex polymer melt flows using the eXtended Pom-Pom model. Journal of Non-Newtonian fluid mechanics, 2002. **108**(1–3): 301–326.
37. Verbeeten W.M.H., Peters G.W.M., Baaijens F., Numerical simulations of the planar contraction flow for a polyethylene melt using the XPP model. Journal of Non-Newtonian fluid mechanics, 2004. **117**(2–3): 73–84.
38. van Os R.G.M., Phillips T.N., Efficient and stable spectral element methods for predicting the flow of an XPP fluid past a cylinder. Journal of Non-Newtonian Fluid Mechanics, 2005. **129**(3): 143–162.
39. Aguayo J.P., Tamaddon-Jahromi H.R., Webster M.F., Extensional response of the pom-pom model through planar contraction flows for branched polymer melts. Journal of Non-Newtonian fluid mechanics, 2006. **134**(1–3): 105–126.
40. Li X.K., Han X.H., Wang X.P., Numerical modeling of viscoelastic flows using equal low-order finite elements. Computer Methods in Applied Mechanics and Engineering, 2010. **199**(9–12): 570–581.
41. Pichelin E., Coupez T., Finite element solution of the 3D mold filling problem for viscous incompressible fluid. Computer Methods in Applied Mechanics and Engineering, 1998. **163**(1–4): 359–371.
42. Cao W., Shen C.Y., Wang R., 3D Flow Simulation of Injection Molding with Iterative Method. Chinese Journal of Applied Mechanics, 2005. **22**(3): 452–455.
43. Nassehi V., Wiley J., Practical aspects of finite element modelling of polymer processing. 2002, Chichester: John Wiley & Sons.
44. Dussan E.B., On the spreading of liquids on solid surfaces: static and dynamic contact lines. Annual Reviews of Fluid Mechanics, 1979. **11**(1): 371–400.
45. Hocking L.M., A moving fluid interface on a rough surface. Journal of Fluid Mechanics, 1976. **76**(04): 801–817.
46. Huh C., Mason S.G., Effects of surface roughness on wetting (theoretical). Journal of Colloid and Interface Science, 1977. **60**(1): 11–38.
47. Silliman W.J., Scriven L.E., Separating how near a static contact line: Slip at a wall and shape of a free surface. Journal of Computational Physics, 1980. **34**(3): 287–313.
48. Navier C., Mémoire sur les lois du mouvement des fluides. Mém l'Acad Roy Sci l'Inst France, 1822. **6**(2): 375–394.
49. Wu C.W., Sun H.X., Quadratic programming algorithm for wall slip and free boundary pressure condition. Journal for Numerical Methods in Fluids, 2006. **50**(2): 131–145.
50. Wu C.W., Hu L.C., Wall slippage and oil film collapse. Journal of Dalian University of Technology, 1993. **33**(2): 172–178.
51. Thompson P.A., Troian S.M., A general boundary condition for liquid flow at solid surfaces. Nature, 1997. **389**: 360–362.
52. Priezjev N.V., Troian S.M., Molecular origin and dynamic behavior of slip in sheared polymer films. Physical review letters, 2004. **92**(1): 18302.